

CR-184197 . 5

FINAL REPORT

NASA/MSFC CONTRACT No. H80589B

PERIOD OF CONTRACT: 5/1/89 - 1/31/90



University of Alabama at Birmingham
Department of Physics
Birmingham, AL 35294

**DESIGN AND ANALYSIS OF MULTILAYER
X-RAY/XUV MICROSCOPE**

DAVID L. SHEALY

PRINCIPAL INVESTIGATOR

FINAL REPORT

TITLE: Design and Analysis of Multilayer X-Ray/XUV Microscope

PRINCIPAL INVESTIGATOR: David L. Shealy, Ph.D.
Department of Physics
University of Alabama at Birmingham
Birmingham, AL 35294
205-934-8068
FAX: 205-934-8042
BITNET: UABDLS01@ASNUAB

CONTRACT NO.: NASA-PO-H80589B

DATE: April 1, 1990

DISTRIBUTION: NASA/MSFC
CODE: CN22D (5)
AT01 (1)
AP29-Q (1)
CC01/Sheehan (1)
EM13B-34 (1)
NASA Scientific and Technical Info. Facility (2)
ES52/Hoover (9)
DCAS/AFPO/NAVPRO (1)
Marshall Space Flight Center, AL 35812

ABSTRACT

Work under this contract has focused on the design and analysis of a large number of normal incidence multilayer x-ray microscopes based on the spherical mirror Schwarzschild configuration. ^{THIS IS EXAMINED.} Design equations for the spherical mirror Schwarzschild microscope ^{WERE} have been summarized and used to evaluate mirror parameters for microscopes with magnifications ranging from 2 to 50x. Ray tracing and diffraction analyses ^{WERE} have been carried out for many microscope configurations to determine image resolution as a function of system parameters. The results are summarized in three publications included in this report. For 10, 20, and 30x ^{WELL} microscopes, construction parameters have been generated and provided to NASA/MSFC PI(R. B. Hoover). A preliminary study of advanced reflecting microscope configurations, where aspherics are used in place of the spherical microscope mirror elements, has indicated that the aspherical elements will improve off-axis image resolution and increase the effective field of view.

RESULTS

Work associated with this contract has resulted in three publications. The paper entitled "Design of a normal incidence multilayer imaging x-ray microscope" by D. L. Shealy, D. R. Gabardi, R. B. Hoover, A. B. C. Walker, Jr., J. F. Lindblom, and T. W. Barbee, Jr. appeared in the J. of X-Ray Science and Technology 1, 190-206 (1989) [enclosed in Appendix A and will be referred to as Paper A in this report]. Paper A described the first demonstration of a two mirror, multilayer soft x-ray instrument to produce high quality images [see Walker, et al., Science 241, 1781 (1988) for more details] and presented the equations and results of a ray trace analysis of a Schwarzschild imaging microscope. Preliminary plans to build a 10.75x Schwarzschild x-ray microscope are given in Paper A. Initially, plans to fabricate a x-ray microscope were constrained by substrate vendors not being able to produce convex spherical secondary mirrors with a radius of curvature less than 15 cm with very smooth surfaces for multilayer coatings. Diffraction calculations of the point spread function of the 10x microscope indicated that an on-axis object plane resolution of 600 Angstroms should be achieved from the spherical Schwarzschild microscope at an operating wavelength of 100 Angstroms.

The second paper associated with this work is entitled "Development of a normal incidence multilayer, imaging x-ray microscope" by D. L. Shealy, R. B. Hoover, A. B. C. Walker, Jr., and T. W. Barbee, Jr. and appeared in the Proc. SPIE 1160, 109-121

(1989) [enclosed in Appendix B and will be referred to as Paper B in this report]. Paper B was presented to the 33rd Annual International Technical Symposium of the SPIE in San Diego, California, August 6-11, 1989, and was distributed by NASA/MSFC Space Science Laboratory, Preprint Series No. 89-123, June, 1989. As a result of advances in substrate fabrication technologies, these investigators recognized that super smooth convex spherical substrates could be produced with a very short radius of curvature of the order of 8 cm. Therefore, it would be practical to build a larger magnification microscope with a shorter overall length. In Paper B, the design parameters of a 20x microscope with an overall length of 1.34m are given in Table 2. This 20x microscope is currently being made with NASA MSFC support in the Space Science Lab. Extensive ray tracing and diffraction analyses for this 20x microscope are given in Paper B. From these studies, one can expect the limit of resolution of this microscope to be about 400 Angstroms in the object plane for a 1 mm full field of view for operations at 125 Angstroms light. To detect this level of resolution will require the use of film with a grain size of 1300 lines per mm over a 20 mm diameter region. Based on developments relating to the Stanford/MSFC Multi-Spectral Solar Telescope Array (MSSTA), the investigators are confident that this 20x microscope can be fabricated, aligned, and tested with soft x-rays using new emulsions and ultra fine-grain developers that should enable resolution test to be limited by the optics - not the detectors.

The third paper produced by this work is entitled "Design and analysis of a Schwarzschild imaging multilayer x-ray microscope" by

D. L. Shealy, R. B. Hoover, T. W. Barbee, Jr., and A. B. C. Walker, Jr. and is scheduled to appear in a special issue of Optical Engineering on x-ray optics in June, 1990. A preprint of this Optical Engineering paper is enclosed in Appendix C and will be referred to as Paper C. Paper C reports extensive calculations of the diffraction modulation transfer function (MTF) for Schwarzschild microscopes with magnifications varying from 2 to 50x. Since for x-ray microscopy applications one is interested in resolving small features within a larger field of view of an extended object, the diffraction MTF is the most appropriate merit function for evaluating system resolution. In order to provide resolution results useful for a number of applications, contrast levels of 20%, 40%, and 60% have been studied. From Fig. 6 of Paper C, one concludes that a Schwarzschild microscope should have a 600 Angstrom spatial resolution in the object plane over an object field of 0.7 mm using a detector that can operate with a 20% MTF. Assuming that a grain size of 1 micron is used as a detector, then a magnification of 20x is required to achieve a resolution less than 0.1 microns over a 0.7 mm field of view. Using a secondary mirror with radius of curvature of 8 cm, then the overall length of this microscope will be 1.34 m, where the system parameters are given in Table 2 of Paper C.

In addition to the results contained in these three papers, a 30x microscope has been optimized to yield minimum object plane resolution as a function of the NA of the primary based on diffraction MTF calculations. Also, the performance of a 10.75x aspherical microscope has been analyzed. More details of these

results are given below.

Schwarzschild Microscope, 30x:

In order to potentially resolve smaller object features with 1 micron grain size film, it is planned to build and test a 30x microscope using a convex secondary mirror with a 8 cm radius of curvature. Scaling the Schwarzschild mirror parameters from Table 1 of Paper C by 0.8 gives the following parameters for a 30x microscope:

Primary Mirror

| | |
|---------------------|----------|
| Radius of Curvature | 22.27 cm |
| Outside Diameter | 8.0 cm |
| Hole Diameter | 2.0 cm |

Secondary Mirror

| | |
|-----------------------------------|-----------|
| Radius of Curvature | 8.0 cm |
| Outside Diameter | 1.76 cm |
| Object Distance from Secondary(s) | 14.451cm |
| Mirror Spacing (d) | 14.270cm |
| Image Distance from Primary(Z) | 170.841cm |

The mirror and hole diameters given above have been determined to minimum vignetting of rays while constraining off-axis aberrations. Recognizing that diffraction theory for an aberration free system predicts that the resolution of a microscope should decrease with

increasing NA, numerous MTF calculations have been done to determine the primary mirror NA which produces minimum image plane resolution for a 30x Schwarzschild microscope. From Fig. 1, the minimum image plane resolution occurs for a primary NA of 0.139. The rapid increase in image resolution for larger NA's result from the increased aberrations of the off-axis rays. Figure 2 displays the MTF and through focus shift for the above 30x microscope on the paraxial image plane. As can be seen in the through focus shift plot of Fig. 2, an improved off-axis resolution can be achieved by defocusing the image plane by about 1 mm. Ray tracing analyses have shown that the above mirror and hole diameters do not produce any vignetting of rays for a 1 mm field of view. This investigator recommends fabrication of the above 30x microscope and the 20x microscope described in Table 2 of Paper C.

Two Mirror Aplanatic Microscope:

In 1957, A. K. Head published [Proc. Phys. Soc LXX, 10-B, 945-949 (1957)] an exact solution of a two mirror microscope which satisfies the Abbe Sine Condition and the constant optical path length condition for finite object and image points. The nonlinear solutions of the equations predict the shapes of the primary and secondary mirror surfaces which will reflect light from the object to image point with constant optical path length for all pupil coordinates. Also, the Abbe Sine Condition is satisfied for all rays. The resulting image will be free of all orders of spherical aberration and coma. However, field curvature will still limit the field of view. In order to obtain some preliminary information of

the potential performance of a Head microscope, the mirror surface coordinates for a 10.75x Head microscope were evaluated and were fit by a linear least squares technique to a conic plus aspherical terms equation for the primary and secondary mirrors. This Head microscope should have similar axial performance as the 10.75x Schwarzschild microscope reported in Paper A. Figure 3 presents a diffraction MTF over the paraxial image plane and a through focus shift. Although these results are preliminary and are not intended to represent a definitive comparison between the performance of a Head and Schwarzschild configuration, it is clear that the Head microscope has better off-axis performance than the Schwarzschild configuration as shown in Figs. 2 and 3 of Paper C. A more definitive comparison of the performance of the Head and Schwarzschild microscopes is planned for 1990. Also, one must take special precautions to be certain that a good representation of the Head mirror surfaces is obtained. After further study of the Head microscope, it is recommended that several Head microscopes be fabricated and tested.

Schwarzschild Microscope, 30x

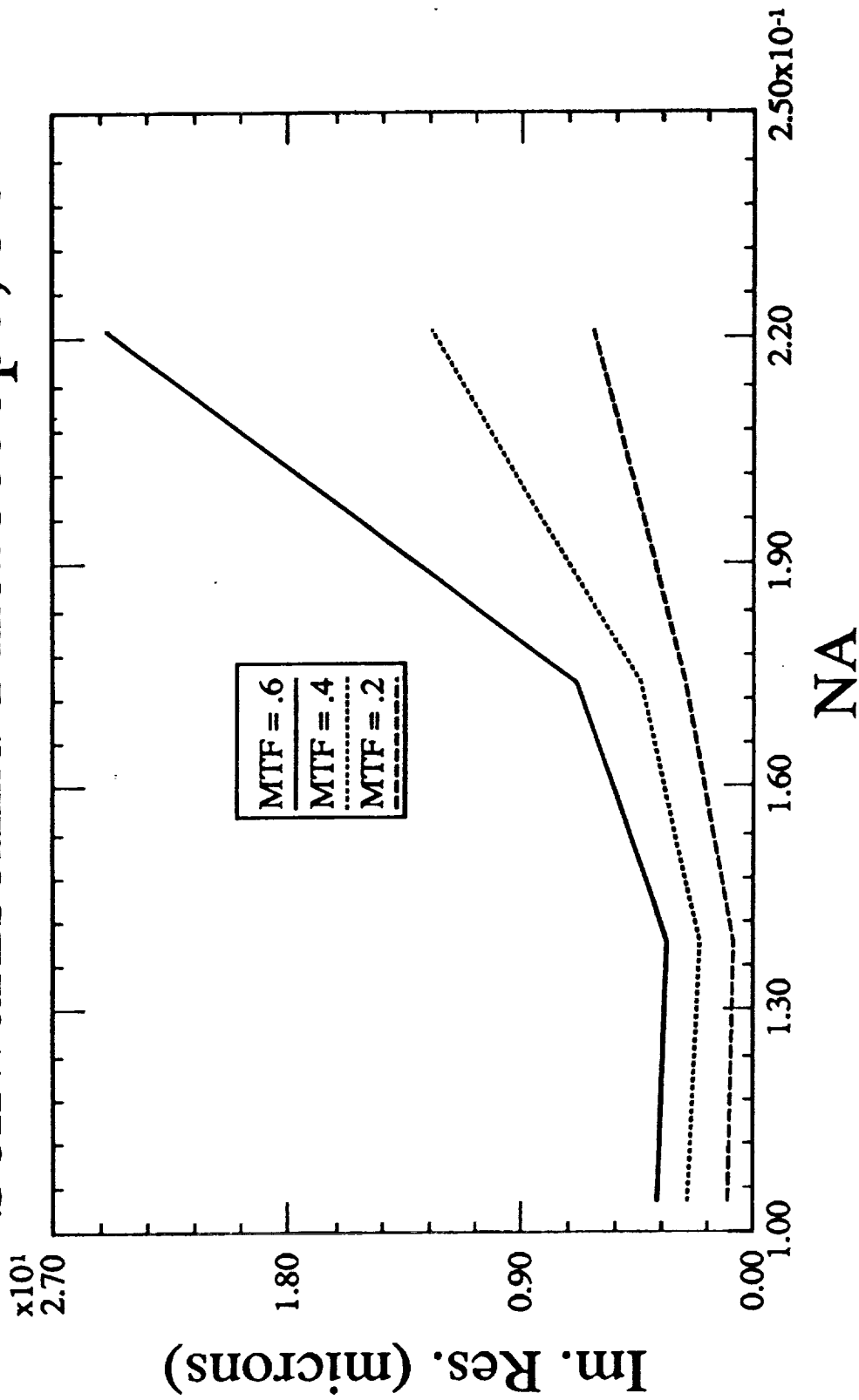


Fig. 1. Paraxial image plane resolution versus the numerical aperture (NA) of the primary for an on-axis object point for 100 Angstrom light.

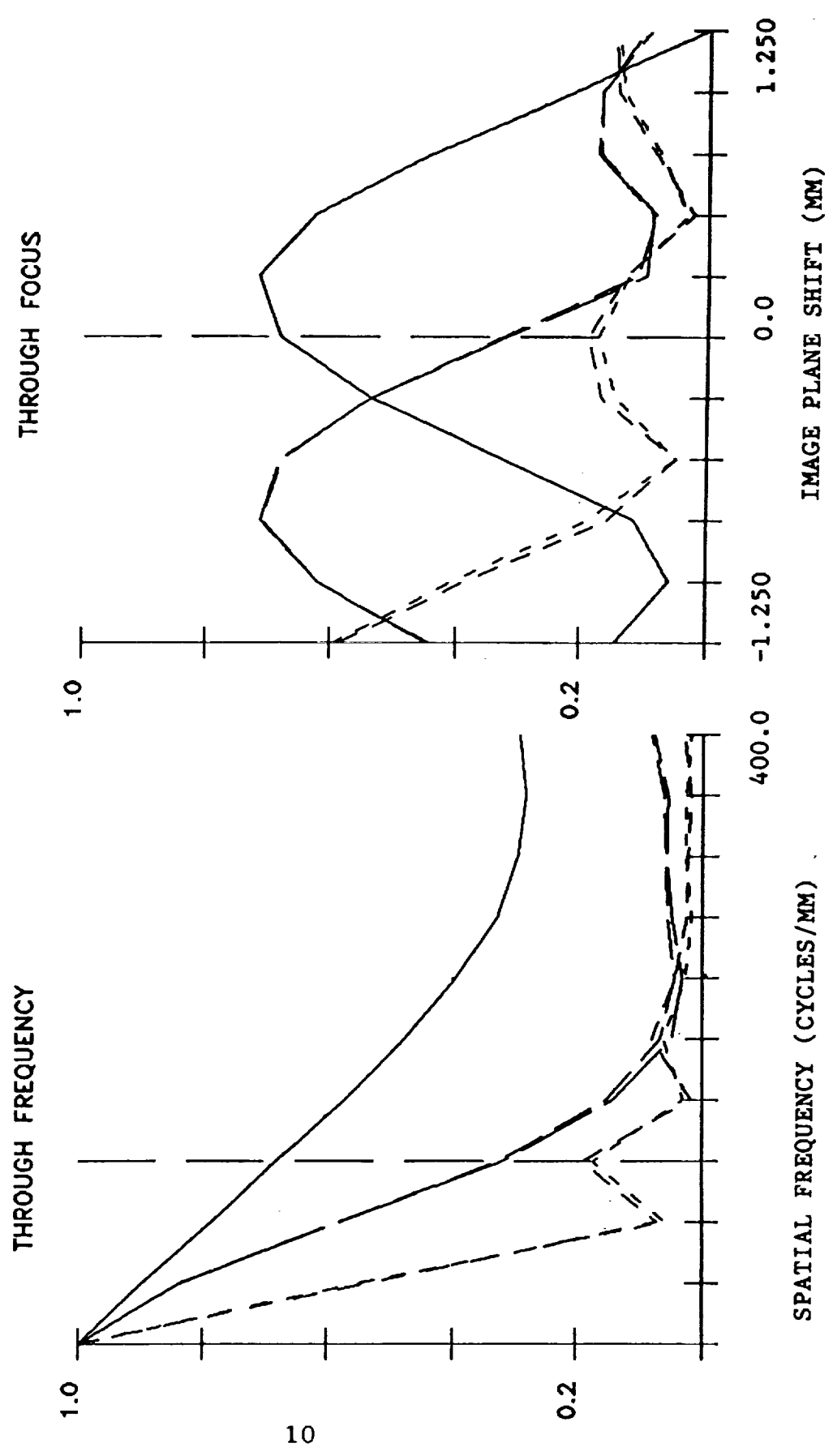
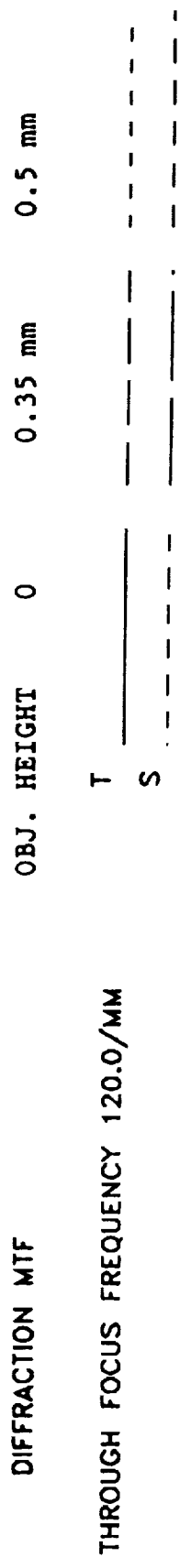


Fig. 2. Diffraction MTF of a 30x spherical Schwarzschild microscope over the paraxial image plane for an on axis object point for 100 Angstrom light.

MODULATION TRANSFER FUNCTION

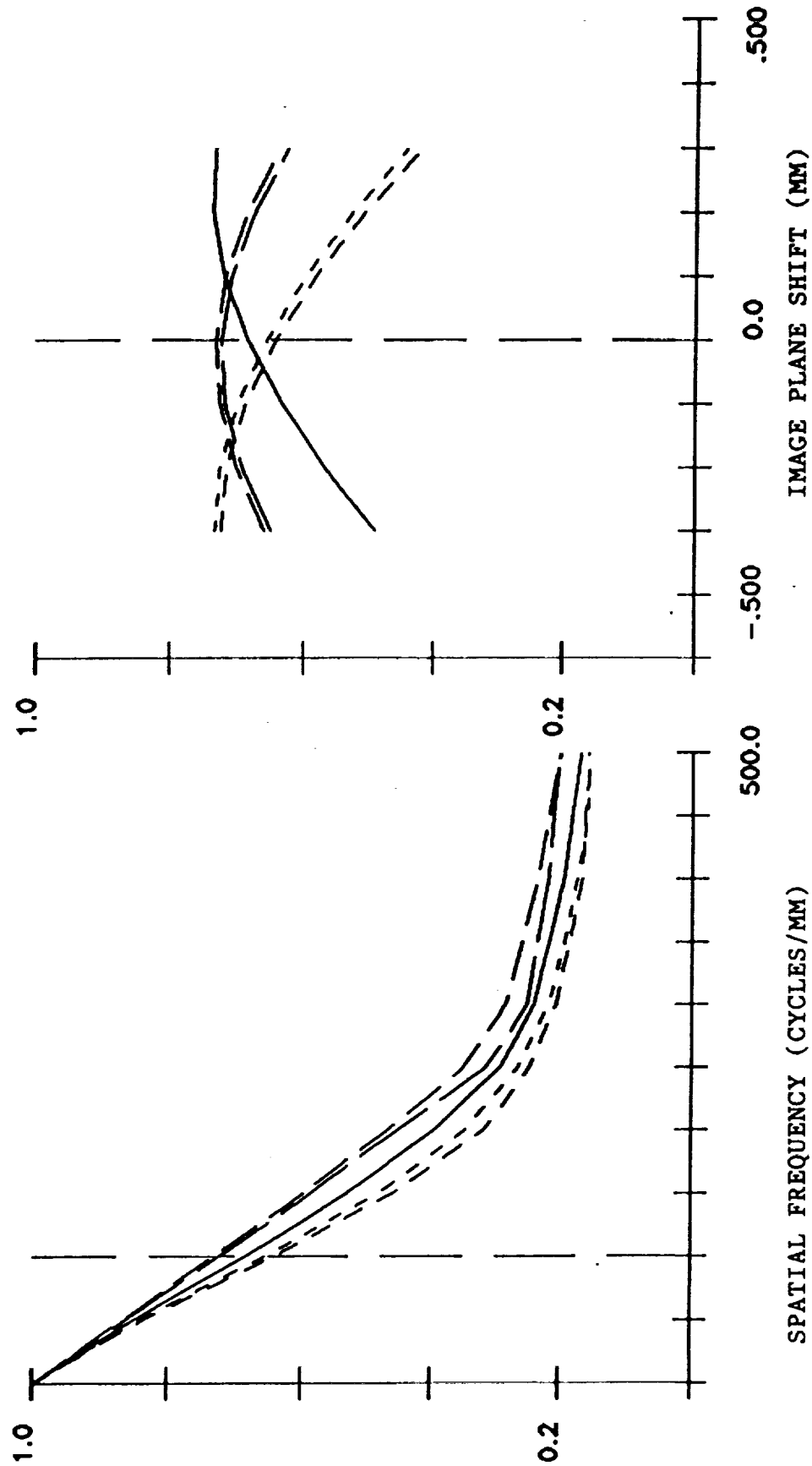
OBJ. HEIGHT 0 0.7 mm 1 mm

THROUGH FOCUS FREQUENCY 100.0/MM



THROUGH FREQUENCY


THROUGH FOCUS



SPATIAL FREQUENCY (CYCLES/MM)

Fig. 3. Diffraction MTF of a 10.75x Head microscope over the paraxial image plane for an on axis object point for 100 Angstrom light.

FORMS

|  | | Report Documentation Page | |
|---|--|--|--|
| 1. Report No. | | 2. Government Accession No. | |
| 3. Recipient's Catalog No. | | 4. Title and Subtitle | |
| Design and Analysis of Multilayer X-Ray/XUV Microscope | | 5. Report Date | |
| | | April 1, 1990 | |
| 6. Performing Organization Code | | 7. Author(s) | |
| | | David L. Shealy | |
| 8. Performing Organization Report No. | | 9. Performing Organization Name and Address | |
| | | Department of Physics University of Alabama at Birmingham Birmingham, AL 35294 | |
| 10. Work Unit No. | | 11. Contract or Grant No. | |
| | | H80589B | |
| 12. Sponsoring Agency Name and Address | | 13. Type of Report and Period Covered | |
| NASA/MSFC Space Sciences Lab, ES-52 Marshall Space Flight Center, AL 35812 | | Final Report 5/1/89-1/31/90 | |
| 14. Sponsoring Agency Code | | 15. Supplementary Notes | |
| | | | |
| 16. Abstract | | | |
| Work under this contract has focused on the design and analysis of a large number of normal incidence multilayer x-ray microscopes based on the spherical mirror Schwarzschild configuration. Design equations for the spherical mirror Schwarzschild microscope have been summarized and used to evaluate mirror parameters for microscopes with magnifications ranging from 2 to 50x. Ray tracing and diffraction analyses have been carried out for many microscope configurations to determine image resolution as a function of system parameters. The results are summarized in three publications included in this report. For 10, 20, and 30x microscopes, construction parameters have been generated and provided to NASA/MSFC PI (R.B. Hoover). A preliminary study of advanced reflecting microscope configurations, where aspherics are used in place of the spherical microscope mirror elements, has indicated that the aspherical elements will improve off-axis image resolution and increase the effective field of view. | | | |
| 17. Key Words (Suggested by Author(s)) | | 18. Distribution Statement | |
| x-ray microscope multilayer | | Unclassified-Unlimited | |
| 19. Security Classif. (of this report) | | 20. Security Classif. (of this page) | |
| none | | none | |
| 21. No. of pages | | 22. Price | |
| 12 plus appendices | | | |

NASA FORM 1028 OCT 88

APPENDIX A

"Design of a Normal Incidence Multilayer Imaging X-Ray Microscope"

David L. Shealy, David R. Gabardi, Richard B. Hoover,
Arthur B.C. Walker, Jr., Joakim F. Lindblom,
and Troy W. Barbee, Jr.

Journal of X-Ray Science and Technology 1, 190-206 (1989)

Design of a Normal Incidence Multilayer Imaging X-Ray Microscope¹

DAVID L. SHEALY,* DAVID R. GABARDI,* RICHARD B. HOOVER,†
ARTHUR B. C. WALKER, JR.,‡ JOAKIM F. LINDBLOM,‡
AND TROY W. BARBEE, JR.§

*Department of Physics, University of Alabama at Birmingham, Birmingham, Alabama 35294;

†Space Science Laboratory, NASA Marshall Space Flight Center, Huntsville, Alabama 35812;

‡Center for Space Science and Astrophysics, Stanford University, Stanford, California 94305;

and §Lawrence Livermore National Laboratory, Livermore, California 94550

Received February 27, 1989; revised September 8, 1989

Normal incidence multilayer Cassegrain x-ray telescopes were flown on the Stanford/MSFC Rocket X-Ray Spectroheliograph. These instruments produced high spatial resolution images of the Sun and conclusively demonstrated that doubly reflecting multilayer x-ray optical systems are feasible. The images indicated that aplanatic imaging soft x-ray/EUV microscopes should be achievable using multilayer optics technology. We have designed a doubly reflecting normal incidence multilayer imaging x-ray microscope based on the Schwarzschild configuration. The Schwarzschild microscope utilizes two spherical mirrors with concentric radii of curvature which are chosen such that the third-order spherical aberration and coma are minimized. We discuss the design of the microscope and the results of the optical system ray trace analysis which indicates that diffraction-limited performance with 600 Å spatial resolution should be obtainable over a 1 mm field of view at a wavelength of 100 Å. Fabrication of several imaging soft x-ray microscopes based upon these designs, for use in conjunction with x-ray telescopes and laser fusion research, is now in progress. High resolution aplanatic imaging x-ray microscopes using normal incidence multilayer x-ray mirrors should have many important applications in advanced x-ray astronomical instrumentation, x-ray lithography, biological, biomedical, metallurgical, and laser fusion research. © 1989 Academic Press, Inc.

1. INTRODUCTION

The development of imaging x-ray microscopes and x-ray telescopes has progressed along very similar avenues, from pinhole cameras to grazing incidence optics of Kirkpatrick-Baez and Wolter configurations. The earliest form of x-ray microscopy, contact microradiography, began shortly after the discovery of x rays in 1896. In contact microradiography the specimen is placed in direct contact with a high resolution photographic plate or an x-ray resist and exposed to x rays. After the plate or resist is developed, the radiographic image is magnified and examined with conventional optical or electron microscopes. Cosslett and Nixon (1) and Howells *et al.* (2) provide a detailed description of the early history of x-ray microscopy. Cosslett developed projection x-ray microscopy techniques, in which the object is placed near

¹ An earlier version of this paper appeared in *Proc. SPIE* 984, 234 (1988).

a point source of x rays and the magnified image is recorded on a distant photographic plate. Pinhole cameras have been used in x-ray microscopy for direct imaging. A pinhole can also be used to restrict the x-ray beam for scanning x-ray microscopes (3). In 1960, Friedman (4) used a pinhole camera to produce the first x-ray image of the Sun. However, these methods have been largely supplanted in observational x-ray astronomy by the use of focusing optical systems. Focusing systems yield larger collecting areas, allow the use of small detectors, and afford significantly enhanced signal-to-noise ratios and spatial resolution. Recently developed normal incidence multilayer x-ray optical systems have been effectively used in x-ray astronomical research. Multilayer optics may be of great value for the production of high resolution aplanatic imaging x-ray microscopes.

In 1948, Kirkpatrick and Baez (5) investigated the possibility of using the principle of x-ray reflection at grazing incidence to produce an x-ray imaging system. They showed that by using a thin curved mirror followed by an identical mirror at right angles to the first, an x-ray optical system corrected for astigmatism could be produced. Kirkpatrick and Pattee (6) studied these systems for the fabrication of reflection x-ray microscopes. The Kirkpatrick-Baez configuration was also adopted by x-ray astronomers. The first image of a cosmic x-ray source (the Cygnus Loop) was produced by a Kirkpatrick-Baez telescope (7, 8). Modular arrays of reflectors allow very large collecting area Kirkpatrick-Baez imaging systems to be made. Telescopes of the Kirkpatrick-Baez configuration, such as the LAMAR instrument (9), are still being developed for large collecting area systems designed for modest resolution imaging and spectroscopic observations of faint sources. LAMAR has recently been selected for flight on the U.S. Space Station *Freedom*.

Several researchers have made Kirkpatrick-Baez x-ray microscopes for investigations of laser fusion plasmas. Seward *et al.* (10) constructed several Kirkpatrick-Baez x-ray microscopes to simultaneously obtain multiple images of an imploding target. By the use of different mirror materials and grazing angles for the reflectors, with properly selected thin metal foil filters, they were able to establish the thermal parameters of the imploding plasma with moderate resolution. Underwood *et al.* (11) have coated a Kirkpatrick-Baez x-ray microscope with multilayers to produce an instrument capable of imaging x rays of 1.54 Å wavelength. However, the spatial resolution of Kirkpatrick-Baez x-ray microscopes has typically been limited to around 1 μm due to x-ray scattering, mirror surface figure errors, and residual optical aberrations. It is interesting that in addition to grazing incidence mirrors, Baez (12) also explored zone plates for image formation in x-ray microscopy. Zone plates have subsequently become a useful tool for imaging x-ray microscopy (13, 14), although their applications in x-ray astronomy have to date been limited.

In 1952, Hans Wolter (15) of Kiel University investigated conic sections of revolution for use at grazing incidence to yield aplanatic x-ray imaging systems. Wolter mirror configurations have found wide applications in both solar and cosmic x-ray astronomy. The Wolter Type I system, which consists of a grazing incidence, internally reflecting paraboloidal mirror followed by a coaxial and confocal internally reflecting hyperboloidal element, has become the most frequently utilized instrument for high resolution imaging in the soft x-ray regime (3–100 Å). The Wolter Type II mirror, in which the second element is an externally reflecting hyperboloidal mirror,

has been widely used in the EUV (100–1000 Å) regime. (See Hoover *et al.* (16) and Underwood and Attwood (17) for a discussion of Wolter telescope configurations.)

Within the past few years, Wolter x-ray microscope configurations have been studied for applications in x-ray astronomy. The attraction of these hybrid systems arises from the fact that x-ray telescope resolution has heretofore been limited by the detector rather than the optics. This problem is even more acute for systems carried aboard satellites, where high resolution photographic films are unfeasible and electronic detectors such as CCDs, MAMAs, etc., must be used. An x-ray microscope can be used to couple the telescope image to the detector to yield a very large plate scale with a telescope that is sufficiently short that it fits within the satellite envelope. Moses *et al.* (18) studied an externally reflecting hyperboloid–hyperboloid x-ray microscope optic and found it to yield 1 arc sec resolution over a very limited field of view (1.25 arc min radius). Hoover *et al.* (19) investigated a grazing incidence x-ray microscope using an internally reflecting hyperboloidal mirror followed by an internally reflecting ellipsoidal element for coupling a Wolter Type I mirror to a detector. This system is also restricted to very limited fields of view (a few arc minutes) due to degradation from off-axis aberrations and vignetting effects (20).

For intense x-ray sources of small angular subtense, however, Wolter grazing incidence x-ray microscopes offer considerable promise. Laser fusion researchers (21, 22) have used Wolter Type I x-ray microscopes to image imploding targets. A hyperboloidal–ellipsoidal grazing incidence x-ray microscope was fabricated by Franks and Gale (23). This 22× system was also configured for laser fusion research and operated at a grazing angle of 1°. Their experimental results indicated that a spatial resolution of about 1 μm was achieved. The performance was limited by optical aberrations and a very low contrast in the image resulting primarily from x-ray scattering effects. They point out that for a grazing incidence system of this focal length to achieve spatial resolution of 0.1 μm, the intensity of the scattered radiation must “be small at angles no greater than 0.0015 arc sec!” This high sensitivity to x-ray scattering coupled with the propensity for grazing incidence x-ray optical systems to scatter x-radiation may be the most serious drawback of Wolter x-ray microscopes.

In astronomy, grazing incidence x-ray microscopes can be of value when coupled to x-ray telescopes for imaging small solar active regions or very bright cosmic sources or for feeding spectrometers. However, their severe off-axis vignetting and aberration effects, as well as the enhanced x-ray scattering effects, prevent grazing incidence microscopes from being useful for applications which require good performance over large fields of view. In contrast, normal incidence multilayer x-ray microscopes do not degrade so rapidly off-axis and are not nearly as subject to the effects of x-ray scattering as are grazing incidence x-ray microscopes. They could be used aft of the focal plane of grazing incidence telescopes to improve both the spectral and spatial resolution of the telescope and allow a variable field of view when used with a fixed detector configuration.

We have recently developed and flown a normal incidence multilayer x-ray telescope to produce high resolution soft x-ray/EUV images of the Sun. The optical system of this telescope is quite similar to that which would be required for a high resolution aplanatic x-ray microscope. It is important to note that the solar x-ray images obtained at 173 Å show virtually *no x-ray scattering*, which suggests that su-

perb x-ray microscopes may also be obtained by the use of multilayer x-ray optical systems. The initial plans for these x-ray microscopes are for use in conjunction with grazing incidence or normal incidence multilayer x-ray telescopes or for imaging laser fusion plasmas. Hence, the source will be observed in emission, and it will be relatively small and of high intensity at the wavelength of interest. Since the soft x-ray/EUV wavelengths for which the normal incidence multilayer optical systems are designed to operate are readily absorbed in air, all microscope components must be designed for operation within a vacuum.

2. STANFORD/MSFC CASSEGRAIN X-RAY TELESCOPE

The first high resolution soft x-ray/EUV images of the Sun with normal incidence multilayer x-ray telescopes were obtained by the Stanford/MSFC Rocket X-Ray Spectroheliograph. Arthur B. C. Walker, Jr., of Stanford University is Principal Investigator; Richard B. Hoover of MSFC, Troy W. Barbee, Jr., of Lawrence Livermore National Laboratory, and Joakim F. Lindblom of Stanford served as Co-Investigators. The instrument was launched on a Nike-boosted Black Brant at 18:05 UT, October 23, 1987, from the White Sands Missile Range, New Mexico. Lindblom *et al.* (24) provide a detailed description of this instrument. The high resolution, high density images produced by the 173 Å Cassegrain conclusively demonstrated that high reflectivity multilayers can be produced on both concave and convex substrates, and that the bandpasses of multilayer mirror components can be accurately matched. Since each multilayer optic reflects effectively in only a relatively narrow bandpass, it is essential that the bandpasses of the primary and secondary elements be accurately matched or very low throughput will result.

Multilayer x-ray optics (25) are made by precisely depositing, on extremely smooth substrates, multiple layers of a high-Z diffractor material separated by low-Z spacer material. The coatings behave like synthetic Bragg crystals. X-ray reflectivity is maximized by satisfying the condition for constructive interference as indicated by the Bragg equation, $n\lambda = 2d_{\text{eff}} \sin \theta$, where n is the order of diffraction, θ is the angle of incidence with respect to the surface, d_{eff} is the effective layer-pair thickness (corrected for refraction effects), and λ is the wavelength of the incident radiation. Although only a very small reflectivity occurs at each high-Z/low-Z interface, excellent reflectivities (>40%) can be achieved when many layer pairs are used. Many factors determine the characteristics of the multilayer response to an incident spectrum. The important parameters are the substrate smoothness and figure, thicknesses and uniformity of the component layers; the x-ray optical constants of the component elements; the number of layers in the multilayer; the interface width or abruptness and atomic composition; and the interface roughness.

Three important points should be considered in relationship to reflecting, imaging x-ray microscopes using multilayer mirrors. First, it is now possible to synthesize multilayer structures having useful normal incidence reflectivities at wavelengths of 40 Å or higher. Second, very high quality spheric and aspheric substrates are now commercially available, with substrate surface roughnesses of 1 to 3 Å RMS and the desired figure to better than $\lambda/20$. Third, multilayer reflectivity is the result of an interference process (Bragg diffraction) so that the desired optically reflected intensity

is proportional to the square of the amplitude of the diffracted light. Scattered light adds linearly with intensity so that it is naturally suppressed relative to the desired Bragg reflected light. These three factors indicate that high resolution, low scatter imaging normal incidence multilayer x-ray optic microscopes, which may be used over a broad spectral range, should be obtainable.

The Stanford/MSFC Rocket X-Ray Spectroheliograph also included the Spectral Slicing Telescope (19) which used convex normal incidence multilayer optics to re-image beams from segments of the Wolter-Schwarzschild grazing incidence primary mirror and produced magnified images at 44, 173, and 256 Å. The Wolter-Schwarzschild primary was a diamond turned metal optic, flown in 1983 for stellar spectroscopy, and it exhibited excessively high x-ray scatter. Microstructure "memory" problems are known to affect diamond turned mirrors after vibration. The calibration test and flight images produced by the Spectral Slicing Telescope component apparently have much lower x-ray scatter than the images from the primary mirror alone. We had previously shown that normal incidence optics can improve the optical performance of grazing incidence telescopes by reducing the overall system offense against the Abbé Sine Condition (19, 20, 26). The low x-ray scatter observed in our flight images suggests that multilayer x-ray microscopes may also be far less sensitive to image degradation from scattering than their grazing incidence counterparts.

High resolution images of the Sun were obtained at both 173 and 256 Å with the "Cassegrain" telescopes. These telescopes (Fig. 1) used spherical optics rather than paraboloidal and hyperboloidal elements of true Cassegrains. Spherical elements were selected due to the difficulty at that time of fabricating conic substrates of the exceptionally high quality surface finish needed for multilayer mirror substrates. The concave spherical primary was 6.4 cm diameter and had a 1.2 m radius of curvature. The convex secondary was also spherical of 2.5 cm diameter and 0.5 m radius of curvature. The effective focal length of the system was 2 m, yielding an $f/34$ system. Theoretical ray trace studies showed the optics to be capable of spatial resolution of less than 0.5 arc sec over the entire field of view. Figure 2 shows the predicted performance of the system. The point spread functions were calculated and found to be very sharp (26). However, the flight image spatial resolution was limited by film grain characteristics to the 1.0–1.5 arc sec range. The film grainularity in the Cassegrain images was increased as the film was push-processed in Kodak T-MAX developer to allow faint coronal structures (such as the polar coronal plumes) to be observed. The Herschelien spherical mirror telescope images were developed for minimum grain,

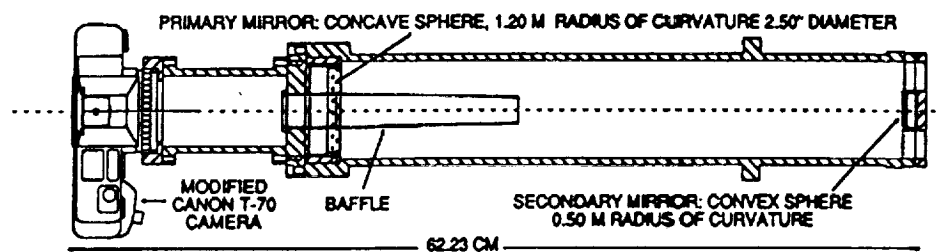


FIG. 1. Schematic of the Stanford/MSFC Normal Incidence Multilayer X-Ray Telescope.

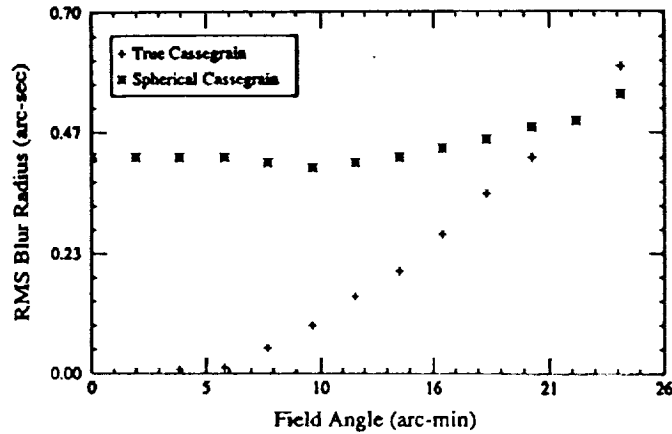


FIG. 2. RMS spot size of normal incidence sphere-sphere "Cassegrain" as compared with the performance of a true Cassegrain.

and clearly reveal that the experimental T-MAX 100 film which was utilized is capable of extremely fine grain and high resolution.

The multilayer optics for the 173 Å instrument were made by coating extremely smooth (<3 Å RMS) substrates with molybdenum/silicon layers of 36.8 and 55.2 Å thickness, respectively (27). The 171–175 Å image shown in Fig. 3 reveals small dark areas in close proximity to very bright active regions. These areas would not be so sharply delineated if significant x-ray scattering were present. In this bandpass, the solar emission is dominated by Fe IX and Fe X lines produced by coronal plasma at 0.95–1.3 million °K. These images show many features of coronal structure, such as magnetically confined loops of hot plasma, prominences and filaments, polar coronal holes, and numerous small discrete supergranulation structures (28). The long exposures show large, faint coronal structures, such as the polar coronal plumes.

Approximately 100 solar x-ray/EUV images were produced by the diverse optical systems on this flight. In addition to demonstrating the value of normal incidence multilayer optics, these images also established that the new experimental tabular grain (T-grain) emulsion, provided by the Eastman Kodak Co., is extremely sensitive over the entire 8 to 256 Å wavelength regime covered by this payload (29). This special film, which has truncated triangular or hexagonal tabular grains, is similar to the Kodak T-MAX 100 emulsion. It was provided without a gelatin overcoat (for maximum sensitivity in the soft x-ray/EUV regimes) and with a Rem-Jet conductive backing (for protection against static discharges after exposure to vacuum). The payload was evacuated prior to launch to prevent acoustic vibrations from destroying the extremely thin filters (1600 Å aluminum on nickel mesh) provided by the Luxel Corp. These highly fragile filters are necessary to allow the soft x-ray/EUV radiation to be efficiently transmitted while reducing the intense visible light from the Sun to sufficiently low levels so that the sensitive film will not be fogged. This flight marked the first successful astronomical use of this important new emulsion. The T-grain



FIG. 3. The solar corona as photographed in the emission of the resonance lines of Fe IX and Fe X at 171 and 174.5 Å, respectively, with a normal incidence Cassegrain multilayer x-ray telescope on the Stanford/MSFC Rocket X-Ray Spectroheliograph. Clearly seen are active regions, loops, prominences, filaments, polar coronal holes, and polar coronal plumes.

emulsions may soon replace the Schumann emulsion technology which has dominated x-ray/EUV astronomical research for the past several decades, and may also be of great value as high resolution, high sensitivity detectors for x-ray microscopy and laser fusion research. Similar x-ray/EUV filters and photographic films will be used in the x-ray microscopes which are now being developed for use with x-ray telescopes and for imaging laser fusion plasmas.

The Stanford/MSFC Multi-Spectral Solar Telescope Array (30), which is being prepared for an early 1990 launch, contains an array of Ritchey-Chretien, Cassegrains, and Herschellian multilayer x-ray/EUV telescopes. An enhanced version of this pay-

load, the Ultra-High Resolution XUV Spectroheliograph (UHRXS) has been selected for flight on the Space Station *Freedom*.

3. RAY TRACE ANALYSIS OF A SCHWARZSCHILD IMAGING MICROSCOPE

Normal incidence multilayer x-ray optics for use in scanning x-ray microscopes have been investigated by Spiller (31) (using an elliptical mirror) and with mirrors of the Schwarzschild configuration by Lovas *et al.* (32) for laser fusion research. Trail and Byer (33) have built a Schwarzschild multilayer optic which has been used to focus the radiation from a laser-induced plasma onto a small spot on a specimen placed in the beam between the optic and the detector. This type of scanning x-ray microscope is intended for biological or metallurgical applications. Other applications of multilayer imaging systems include soft x-ray projection lithography (34).

Since it has been established that high quality multilayers mirrors can be produced on concave and convex spherical substrates, with appropriate bandpass matching to yield high throughput and excellent spatial resolution, we have selected the Schwarzschild configuration for our x-ray microscope design. An aplanatic, two spherical mirror microscope can be constructed by imposing the Schwarzschild Condition (35) on selection of the mirror radii. The Schwarzschild Condition can be understood by referring to Fig. 4.

The mirror surfaces S_1 and S_2 are concentric spherical surfaces of radii R_1 and R_2 , respectively. From the geometry, one can write the following relationships:

$$\sin a = \frac{h}{Z_0} \tag{1a}$$

$$\sin b = \frac{h}{R_1} \tag{1b}$$

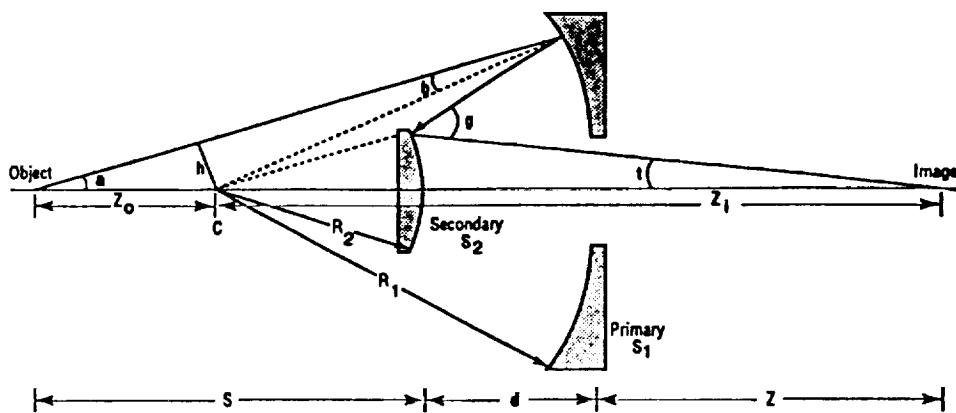


FIG. 4. Schwarzschild configuration for aplanatic normal incidence multilayer x-ray microscope.

$$\sin(0.5g) = \frac{h}{R_2} \quad [1c]$$

$$\sin t = \frac{h}{Z_i} \quad [1d]$$

and

$$t = g - a - 2b. \quad [2]$$

Solving Eqs. [1]–[2] for Z_i , where an expansion through third order for the sine and inverse sine functions has been used, gives the following expression for the image distance Z_i ,

$$Z_i = \left(C_1 + \frac{h^2}{6} [C_2 - C_1^3] \right)^{-1}, \quad [3]$$

where

$$C_1 = \frac{2}{R_2} - \frac{2}{R_1} - \frac{1}{Z_0}$$

$$C_2 = \frac{2}{R_2^3} - \frac{2}{R_1^3} - \frac{1}{Z_0^3}.$$

A minimum for third-order spherical aberration, coma, and the length of the astigmatic lines (36) occurs when the rate of change of the image distance Z_i with respect to the distance h of the ray from the mirrors centers of curvature is equal to zero:

$$\frac{dZ_i}{dh} = 0 = - \left\{ C_1 + \frac{h^2}{6} [C_2 - C_1^3] \right\}^{-2} \times \frac{h}{3} [C_2 - C_1^3]. \quad [4]$$

It should be noted that Eq. [4] does not place any constraint on the aberrations of field curvature, astigmatism, or distortion of the microscope, since these aberrations depend upon the field variable which is the object height. The term within the { } brackets cannot go to infinity. This would occur only when C_1 or C_2 goes to infinity, which will not happen for nonzero R_1 , R_2 , and Z_0 . (If Z_0 were equal to zero, then a real image would not be formed since the object would be at the center of curvature of the mirrors.) Consequently, Eq. [4] can be satisfied only when the term within [] brackets is equal to zero:

$$C_2 - C_1^3 = 0. \quad [5]$$

Equation [5] leads to the Schwarzschild Condition for an aplanatic, two mirror imaging system,

$$\frac{R_2}{R_1} = 1.5 - \frac{R_2}{Z_0} \pm \left[1.25 - \frac{R_2}{Z_0} \right]^{1/2}, \quad [6]$$

where the "+" sign is used in Eq. [6] for magnifications greater than 5, and the "-" sign is used in Eq. [6] for magnifications less than 5. An expression for the magnification will be given below. For this optical system, it can be shown by considering parallel incident light upon the system that the two principal planes (H_1 and H_2) are located at the center of curvature of the two mirrors. The system focal length, f , measured from the principal planes can be written in the form

$$f = \frac{f_1 f_2}{f_1 + f_2 - d}, \quad [7]$$

where $f_1 = 0.5 R_1$, $f_2 = -0.5 R_2$, and d is the mirror separation along the optical axis. Note that both R_1 and R_2 are positive and that the optics sign convention for radii of curvatures has not been used in these equations. The magnification, M , of a two mirror microscope is equal to the product of the magnifications of the primary and secondary mirrors. For the primary, $m_1 = s'_1/s_1$, where the object distance, $s_1 = R_1 + Z_0$, and the image distance, s'_1 , follows from solving the lens equation ($1/s + 1/s' = 1/f$):

$$s'_1 = \frac{R_1(R_1 + Z_0)}{R_1 + 2Z_0}.$$

Then,

$$m_1 = \frac{R_1}{R_1 + 2Z_0}. \quad [8a]$$

For the secondary, the object distance is given by

$$s_2 = -s'_1 + (R_1 - R_2),$$

and the image distance, s'_2 , follows from solving the lens equation:

$$s'_2 = \frac{R_2 s_2}{R_2 + 2s_2}.$$

Then,

$$m_2 = -\frac{R_2(R_1 + 2Z_0)}{2R_1 Z_0 - R_1 R_2 - 2R_2 Z_0}. \quad [8b]$$

The magnification of the two mirror system is then given by

$$M = -\frac{R_1 R_2}{2R_1 Z_0 - R_1 R_2 - 2R_2 Z_0}. \quad [9]$$

Equations [6] and [9] can be used to examine the relationship between M , R_1 , and R_2 for a Schwarzschild imaging microscope. In Table 1, M and R_2 are assumed to be given, and Eqs. [6] and [9] have been solved for R_1 . Table 1 also presents values for the spacings between the object and secondary, $s = Z_0 + R_2$, the secondary and the primary, $d = R_1 - R_2$, and the primary and the image plane, $Z = Z_i - R_1$.

The dimensional quantities in Table 1 scale in a linear manner. For example, if R_2 is increased by a factor "c" to " cR_2 ," then new values for the quantities listed in Table 1 except for M will be obtained by multiplying those values given in Table 1 times "c." It seems practical to construct a microscope with a secondary radius equal to 15 cm. Then, for a 10 \times system, $R_1 = 47.69$ cm, $f = 10.94$ cm, and the total length of the microscope ($s + d + Z$) = 132.47 cm.

The data presented in Table 1 give the mirror radii of curvature and the axial spacings for the object, mirrors, and image plane. In order to make a Schwarzschild microscope, it is also necessary to specify the outside diameter of the mirrors and the diameter of the hole in the primary. A general ray trace analysis has been carried out on a Schwarzschild microscope to fix the diameters of the mirrors and the hole in the primary. Table 2 gives the system parameters of a microscope which has been analyzed in detail.

The data given in Table 2 were selected because they represent a system which can be built with present technology. As a result of the large radii of curvatures, as far as microscope optics go, it is necessary to keep the magnification relatively low in order that the overall length of the system remains manageable. The large primary radius of curvature also requires the distance between the object and primary mirror to be large, which produces a low numerical aperture (NA) for the system that in turn affects the resolution (37). For the microscope given in Table 2, NA = 0.05, and the diffraction-limited resolution is approximately 0.1 μm with 100 \AA light. In contrast to the scanning configuration of Trail and Byer (33) it is thought that successful demonstration of the full field imaging capabilities of an aplanatic microscope similar to that described in Table 2 will provide impetus to produce multilayer mirrors with smaller curvatures, thereby enabling instruments with higher magnification and better resolution to be built. Efforts have been made to arrive at a design which has both a reasonable magnification and resolution and is of the appropriate physical size using optics which can be fabricated with current technology.

TABLE I
Normal Incidence Multilayer Schwarzschild X-Ray Microscopes for Magnifications from 10 \times to 50 \times

| Schwarzschild mirror parameters | | | | | | |
|---------------------------------|------------|------------|----------|----------|----------|----------|
| $M(x)$ | R_1 (cm) | R_2 (cm) | s (cm) | d (cm) | Z (cm) | f (cm) |
| 10 | 31.79 | 10.00 | 18.02 | 21.79 | 48.36 | 7.29 |
| 15 | 29.69 | 10.00 | 18.04 | 19.69 | 91.04 | 7.54 |
| 20 | 28.75 | 10.00 | 18.05 | 18.75 | 131.49 | 7.67 |
| 30 | 27.84 | 10.00 | 18.06 | 17.84 | 213.27 | 7.80 |
| 40 | 27.40 | 10.00 | 18.07 | 17.40 | 296.07 | 7.87 |
| 50 | 27.15 | 10.00 | 18.07 | 17.15 | 376.42 | 7.92 |

TABLE 2
Detailed System Parameters for a 10.75× Schwarzschild X-Ray Microscope

| Schwarzschild microscope system parameters | |
|---|----------|
| Magnification | 10.75 |
| Focal length | 11.0 cm |
| Primary mirror | |
| Radius of curvature | 47.0 cm |
| Outside diameter | 6.4 cm |
| Hole diameter | 2.2 cm |
| Secondary mirror | |
| Radius of curvature | 15.0 cm |
| Outside diameter | 1.6 cm |
| Object distance from secondary (<i>s</i>) | 27.0 cm |
| Mirror spacing (<i>d</i>) | 32.0 cm |
| Image distance from primary (<i>Z</i>) | 82.4 cm |
| Overall length (<i>s</i> + <i>d</i> + <i>Z</i>) | 141.4 cm |

The RMS blur radius as a function of the object height is plotted in Fig. 5a. The image plane is located at the position of best focus for an on-axis object point. This graph indicates diffraction limited performance out to an object height of approximately 0.7 mm. That is, when the object is off-axis by more than 0.7 mm, the image blurring due to optical aberrations becomes larger than that due to diffraction effects for 100 Å light. In actuality, point spread function calculations which have also been carried out have indicated that diffraction limited performance should be achievable over an even larger field of view. The RMS blur radius versus the object height for three different positions of the image plane is shown in Fig. 5b. As indicated, a larger

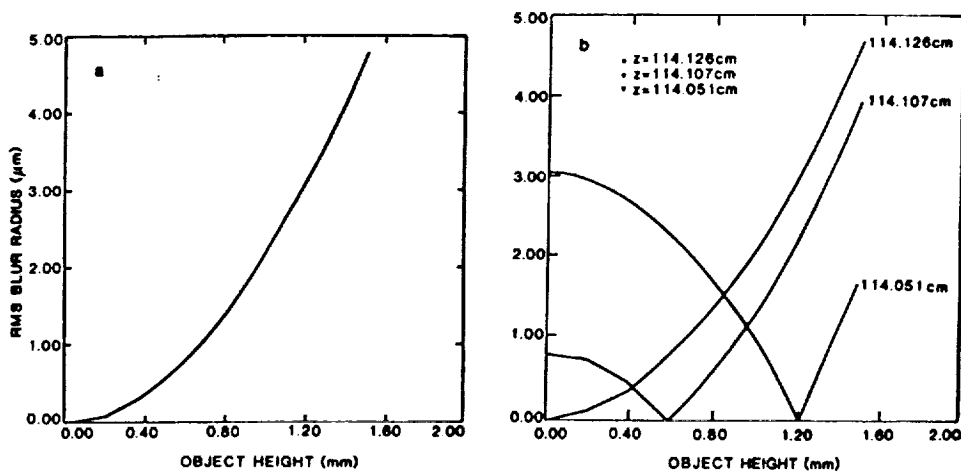


FIG. 5. (a) RMS blur radius vs object height. (b) RMS blur radius over three different image planes vs object height. *z* specifies the image plane to primary mirror distance.

field of view with submicrometer RMS values can be obtained by displacing the image plane about 2 mm toward the primary.

System tolerancing has also been investigated. Figure 6 presents the RMS blur radius versus decentration for independent displacements of the primary and the secondary. The RMS blur radius versus the tilt angle of the primary and secondary mirrors, respectively, is shown in Figs. 7a and 7b, when the mirror vertex is fixed on the optical axis. Image defects due to tilt of the primary mirror are about three times larger than those resulting from secondary mirror tilt, but even these do not pose unacceptable alignment tolerances. Submicrometer resolution can still be obtained for tilts of the primary up to about 1 arc min. With a mounting structure which allows adjustments after assembly of the microscope, these critical alignments can be adequately controlled.

4. X-RAY MICROSCOPE FABRICATION PLANS

Several mirror systems are now being considered for fabrication for use in the 44 to 175 Å regime for astronomical and laser fusion applications. One 14× system utilizes a primary mirror of 6.35 cm diameter with a 50 cm radius of curvature. The primary has a central hole of 2.2 cm diameter. This microscope has a secondary of 1.6 cm diameter with a radius of curvature of 16.7 cm. This configuration yields an x-ray microscope with overall length of approximately 2 m ($s = 30.13$ cm, $d = 33.3$ cm, $Z = 139.6$ cm, and $f = 12.54$ cm). Figure 8 presents the RMS versus object height for this 14× microscope over the image plane with minimum RMS for on-axis point source light ($Z + d = 171.97$ cm). Figure 9 shows the diffraction point

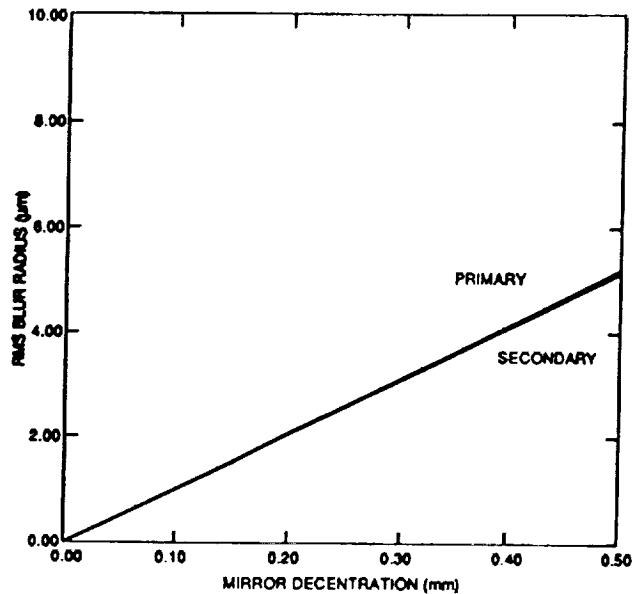


FIG. 6. RMS blur radius vs mirror decentration for independent displacements of the primary and secondary mirrors. The image plane location was varied to obtain minimum RMS values.

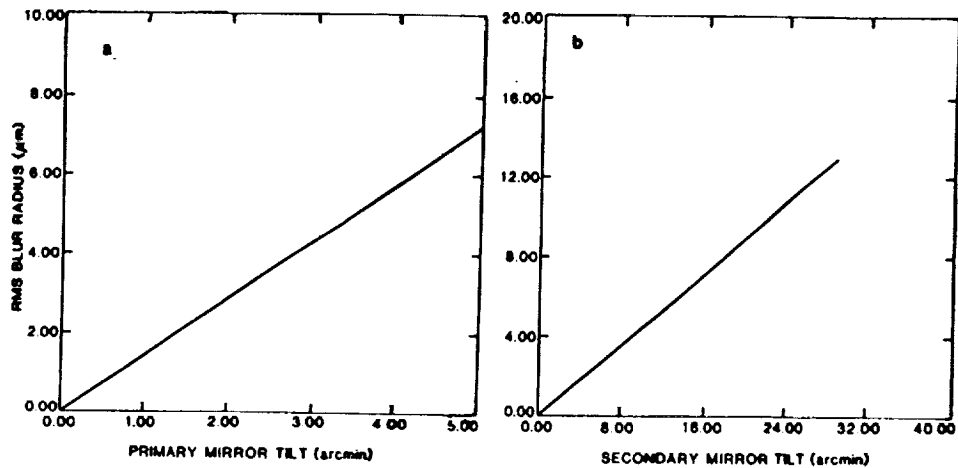


FIG. 7. (a) RMS blur radius vs primary mirror tilt angle where vertex of mirror was fixed on optical axis. (b) RMS blur radius vs secondary mirror tilt angle when the vertex of mirror was fixed on optical axis.

spread function over the same image plane for a 600 \AA diameter source of 100 \AA radiation. The results presented in Fig. 9 were evaluated from the diffraction analysis code *GLAD*. Noting that the grid size used in Fig. 9 is $0.85 \mu\text{m}$, then one can conclude that resolution of 600 \AA in the object plane is possible provided the detector in the image plane permits spatial resolution better than $0.85 \mu\text{m}$.

Several $20\times$ microscopes are also under consideration for fabrication. One system has a total length of 2 m with primary and secondary radii of curvature of 34.21 and 11.9 cm, respectively. Depending on the aperture used for the primary, it is possible based on RMS calculations similar to those shown in Fig. 8 to obtain 600 \AA resolution over a field of view of 1 mm for both the $14\times$ and the $20\times$ systems. We plan to couple the microscopes to 35 mm Canon T-70 cameras, such as were used in the Stanford/MSFC Rocket X-Ray Spectroheliograph payload. Special experimental soft x-ray/

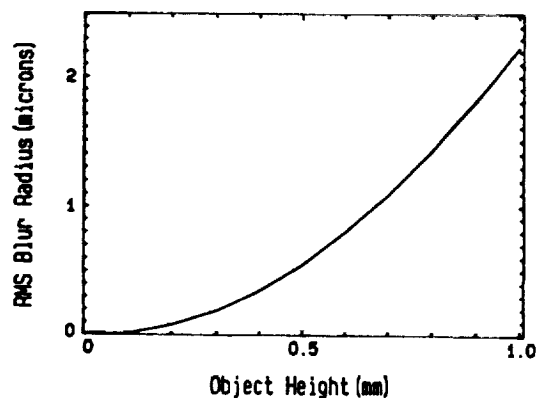


FIG. 8. RMS blur radius vs object height for a $14\times$ microscope with a 2 m overall length.

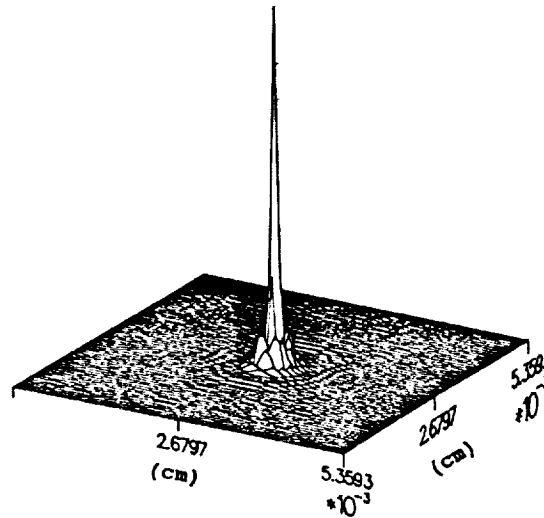


FIG. 9. Point spread function (PSF) over the image plane of a 14 \times microscope using 100 \AA radiation from a 600 \AA diameter source of x rays. The image plane grid units in this figure are 0.8506 μm .

EUV sensitive photographic emulsions of extremely high spatial resolution and excellent sensitivity are planned for use with this new instrument.

5. CONCLUSIONS

The Stanford/MSFC Rocket X-Ray Spectroheliograph solar x-ray images produced with a doubly reflecting Cassegrain using normal incidence x-ray optics configured from extremely smooth spherical substrates have clearly shown that high quality multilayer mirrors can be produced on both convex and concave substrates. The high density observed in the photographic images reveals that excellent soft x-ray/EUV reflectivities are achievable and that accurate matching of the wavelengths of peak reflectivity of the components can be achieved. These results have led us to explore the possibility of producing a high sensitivity, high resolution aplanatic x-ray microscope using normal incidence multilayer mirrors. Our Cassegrain x-ray telescope images and analytical study indicate that soft x-ray/EUV aplanatic imaging multilayer microscopes can be fabricated which will have high throughput and which should be capable of achieving spatial resolution $< 600 \text{\AA}$.

We have designed several microscopes based upon the Schwarzschild configuration and have analyzed microscopes of magnifications ranging from 10.75 \times to 20 \times in detail. The 14 \times system has a diffraction limited resolution of 600 \AA at a wavelength of 100 \AA . We have analyzed the performance as a function of object height and found that diffraction-limited performance extends over at least a 1 mm field of view. Mirror substrates are being manufactured for the fabrication of normal incidence multilayer x-ray microscopes of approximately 2 m overall length and capable of operating at magnifications ranging from 14 \times to 20 \times . The exact multilayer coatings to be utilized will be selected in accordance with the goals of maximizing throughput and resolu-

tion and the nature of the objects or plasma sources to be investigated. High resolution aplanatic imaging x-ray microscopes configured from low x-ray scatter normal incidence multilayer optics should be ideal for laser fusion research, biological investigations, and high spatial resolution astronomical investigations when used in conjunction with grazing incidence or multilayer x-ray telescope systems.

ACKNOWLEDGMENTS

We are deeply grateful to Richard A. Van Patten, John Gill, Russell Hacker, and John Trail of Stanford University, Richard Rakoff, Harry Zimmer, Charles Welch, Jesus Martinez, and Carlos Martinez of the Lockheed SPARCS Office, Gordon Steele of the Luxel Corp., and H. Murray Cleare, Gordon Brown, Martin Scott, and Al DeWan of Eastman Kodak Co. We also thank Mike Hettrick, Chris Kalange, Frank Lau, Donald Patterson, and Tauna Moorehead. The Stanford/MSFC Rocket X-Ray Spectroheliograph Project was funded by NASA Grant NSG5131 and received its initial support through the Center Director's Discretionary Fund of NASA/MSFC. We also express gratitude to the MSFC CDDF Program for the support provided the current x-ray microscope research.

REFERENCES

1. V. E. COSSLETT AND W. C. NIXON, "X-Ray Microscopy," Cambridge Univ. Press, Cambridge, 1960.
2. M. HOWELLS, J. KIRZ, D. SAYRE, AND G. SCHMAHL, *Phys. Today* Aug., 22 (1985).
3. P. HOROWITZ AND J. A. HOWELL, *Science* **178**, 608 (1972).
4. H. FRIEDMAN, *Sky Telescope* **20**, 143 (1960).
5. P. KIRKPATRICK AND A. V. BAEZ, *J. Opt. Soc. Amer.* **38**, 766 (1948).
6. P. KIRKPATRICK AND H. H. PATTEE, JR., in "Handbuch der Physik" (S. Flugge, Ed.), Vol. XXX, Springer-Verlag, Berlin/New York, 1957.
7. P. GORENSTEIN, B. HARRIS, H. GURSKY, R. GIACCONI, AND P. VANDENBOUT, *Science* **172**, 369 (1971).
8. P. GORENSTEIN, B. HARRIS, H. GURSKY, AND R. GIACCONI, *Nucl. Instrum. Methods* **91**, 451 (1971).
9. L. M. COHEN, D. G. FABRICANT, AND P. GORENSTEIN, *Proc. SPIE* **691**, 126 (1986).
10. F. D. SEWARD, J. DENT, M. BOYLE, L. KOPPEL, T. HARPER, P. STOERING, AND A. TOOR, *Rev. Sci. Instrum.* **47**, 464 (1976).
11. J. H. UNDERWOOD, T. W. BARBEE, JR., AND C. FRIEBER, *Appl. Opt.* **25**, 1730 (1986).
12. A. V. BAEZ, *J. Opt. Soc. Amer.* **42**, 756 (1952).
13. G. SCHMAHL, D. RUDOLPH, P. GUTTMANN, AND O. CHRIST, in "X-Ray Microscopy, Proceedings of the International Symposium, Federal Republic of Germany, Sept. 14-16, 1983" (G. Schmahl and D. Rudolph, Eds.), p. 63, Springer-Verlag, Berlin, 1984.
14. H. RARBACK, J. M. KENNEY, J. KIRZ, M. R. HOWELLS, P. CHANG, P. J. COANE, R. FEDER, P. J. HOUZEGO, D. P. KERN, AND D. SAYRE, in "X-Ray Microscopy, Proceedings of the International Symposium, Federal Republic of Germany, Sept. 14-16, 1983" (G. Schmahl and D. Rudolph, Eds.), p. 203, Springer-Verlag, Berlin, 1984.
15. H. WOLTER, *Ann. Phys.* **10**, 94, 286 (1952).
16. R. B. HOOVER, R. J. THOMAS, AND J. H. UNDERWOOD, *Adv. Space Sci. Technol.* **11**, 1 (1973).
17. J. H. UNDERWOOD AND D. T. ATTWOOD, *Phys. Today* **44** (1984).
18. D. MOSES, A. S. KRIEGER, AND J. M. DAVIS, *Proc. SPIE* **691**, 138 (1986).
19. R. B. HOOVER, D. L. SHEALY, AND S. CHAO, *Opt. Eng.* **25**, 970 (1986).
20. D. L. SHEALY AND R. B. HOOVER, *Proc. SPIE* **640**, 28 (1986).
21. R. H. PRICE, in "Low Energy X-Ray Diagnostics" (D. T. Attwood and B. L. Henke, Eds.), *AIP Conf. Proc.* **75**, p. 189, American Institute of Physics, New York, 1981.
22. S. AOKI AND S. KIKUTA, *Japan J. Appl. Phys.* **13**, 1385 (1974).

23. A. FRANKS AND B. GALE, in "X-Ray Microscopy, Proceedings of the International Symposium, Federal Republic of Germany, Sept. 14-16, 1983" (G. Schmahl and D. Rudolph, Eds.), p. 129, Springer-Verlag, Berlin, 1984.
24. J. F. LINDBLOM, A. B. C. WALKER, JR., R. B. HOOVER, T. W. BARBEE, JR., R. A. VANPATTEN, AND J. P. GILL, *Proc. SPIE* **982**, 316 (1988).
25. T. W. BARBEE, JR., *Opt. Eng.* **25**, 898 (1986).
26. D. L. SHEALY, R. B. HOOVER, AND D. R. GABARDI, *Proc. SPIE* **691**, 83 (1986).
27. A. B. C. WALKER, JR., J. F. LINDBLOM, R. B. HOOVER, AND T. W. BARBEE, JR., *J. Phys. Colloq. C1* **49**, 175 (1988).
28. A. B. C. WALKER, JR., T. W. BARBEE, JR., R. B. HOOVER, AND J. F. LINDBLOM, *Science* **241**, 1781 (1988).
29. R. B. HOOVER, T. W. BARBEE, JR., J. F. LINDBLOM, AND A. B. C. WALKER, JR., *Kodak Tech Bits Summer*, 1 (1988).
30. A. B. C. WALKER, JR., J. K. LINDBLOM, R. H. O'NEAL, M. J. ALLEN, T. W. BARBEE, JR., AND R. B. HOOVER, *Proc. SPIE* **1160**, 131 (1989).
31. E. SPILLER, in "X-Ray Microscopy, Proceedings of the International Symposium, Federal Republic of Germany, Sept. 14-16, 1983" (G. Schmahl and D. Rudolph, Eds.), p. 226, Springer-Verlag, Berlin, 1984.
32. I. LOVAS, W. SANTY, E. SPILLER, R. TIBBETS, AND J. WILCZYNSKI, *Proc. SPIE* **316**, 90 (1981).
33. J. A. TRAIL AND R. L. BYER, *Proc. SPIE* **563**, 90 (1985).
34. A. M. HAWRYLUK AND L. G. SEPPALA, *J. Vac. Sci. Technol. B* **6**(6), 2162 (1988).
35. K. SCHWARZSCHILD, *Göttingen Mitt* **10**, 2 (1905).
36. W. J. SMITH, "Modern Optical Engineering," p. 63, McGraw-Hill, New York, 1966.
37. F. JENKINS AND H. WHITE, "Fundamentals of Optics," p. 333, McGraw-Hill, New York, 1976.

APPENDIX B

"Development of a Normal Incidence Multilayer,
Imaging X-Ray Microscope"

David L. Shealy, Richard B. Hoover,
Arthur B.C. Walker, Jr.,
and Troy W. Barbee, Jr.

SPIE Vol. 1160 X-Ray/EUV Optics for Astronomy and Microscopy, 109-
121 (1989)

PROCEEDINGS REPRINT

 SPIE—The International Society for Optical Engineering

Reprinted from

X-Ray/EUV Optics for Astronomy and Microscopy

**7-11 August 1989
San Diego, California**



Volume 1160

©1989 by the Society of Photo Optical Instrumentation Engineers
Box 10, Bellingham, Washington 98227 USA. Telephone 206/676-3290.

DEVELOPMENT OF A NORMAL INCIDENCE MULTILAYER, IMAGING X-RAY MICROSCOPE

David L. Shealy
Dept. of Physics, University of Alabama at Birmingham
Birmingham, Alabama 35294

Richard B. Hoover
Space Science Laboratory, NASA Marshall Space Flight Center
Huntsville, Alabama 35812

Arthur B. C. Walker, Jr.
Stanford University, Stanford, California 94305

Troy W. Barbee, Jr.
Lawrence Livermore National Laboratory
Livermore, California 94550

ABSTRACT

Normal incidence multilayer x-ray mirror technology has now advanced to the point that high resolution x-ray microscopes with relatively large fields of view are feasible. High resolution aplanatic imaging x-ray microscopes configured from low x-ray scatter normal incidence multilayer optics should be ideal for laser fusion research, biological investigations, and for astronomical studies when used in conjunction with grazing incidence or multilayer x-ray telescope systems. We have designed several Schwarzschild x-ray microscope optics. Diffraction analysis indicates better than 400 Å spatial resolution in the object plane up to a 1 mm field of view can be achieved with 125 Å radiation. We are currently fabricating a 20x normal incidence multilayer x-ray microscope of 1.35 meter overall length. We have also analyzed and designed other microscope systems for use in conjunction with x-ray telescopes. We report on the results of these studies and the x-ray microscope fabrication effort.

1. INTRODUCTION

The high resolution, full-disk solar x-ray images produced with the Stanford/MSFC Rocket X-Ray Spectroheliograph clearly demonstrated that doubly reflecting multilayer x-ray imaging systems could be produced.^{1,2} The images obtained with this system show extremely high spatial resolution, and they also reveal that these telescopes have virtually no x-ray scattering. Good full disk solar x-ray images were obtained with the 256 Å Herschelian telescope in exposure times of 0.5 seconds and in 8 second exposures at 44 Å with convex multilayers in the Wolter-Cassegrain component. The densities obtained on the photographic emulsions³ in these short exposures clearly indicate that high reflectivities can be achieved with contoured multilayer optics working at normal incidence. The excellent, high density images produced by the 173 Å Cassegrain⁴ conclusively proved that high reflectivity multilayers can be produced on both concave and convex substrates, and that the bandpasses of multilayer mirror components can be accurately matched. Since each multilayer optic reflects effectively in only a relatively narrow bandpass, it is essential that the bandpasses of the primary and secondary elements be accurately matched or very low throughput will result. Recent tests of this Cassegrain telescope, carried out in collaboration with Barry Welsh at the Space Sciences Laboratory of the University

of California, Berkeley, and Joakim Lindblom of Stanford University, have confirmed that reflection efficiencies for each telescope mirror exceeded 25% at 173 Å.

The multilayer optics for the 173 Å instrument were made by coating extremely smooth (<3 Å rms) substrates with Molybdenum/Silicon layers of 36.8 Å and 55.2 Å thickness, respectively.² The normal incidence multilayer Cassegrain telescopes produced full-disk solar soft x-ray/EUV images with almost no x-ray scattering in the 173 Å and 256 Å regions. The solar images have small dark areas which can be clearly seen in close proximity to very bright active regions. Furthermore, low contrast features, such as polar coronal plumes, can be seen in the images. These features would not be so clearly visible if significant x-ray scattering were present. In the 171-173 Å bandpass, the solar emission is dominated by Fe IX and Fe X lines produced by coronal plasma at 0.95-1.3 million °K.

These exciting results with doubly reflecting multilayer telescopes obtained during the flight of the Stanford/MSFC Rocket X-Ray Spectroheliograph led to the development of an entirely new payload, the Stanford/MSFC Multi-Spectral Solar Telescope Array (MSSTA), which is scheduled for launch from the White Sands Missile Range later this year (see Walker et al.⁵ for a description of this powerful new instrument). These results also encouraged us to continue our efforts to develop an aplanatic imaging x-ray microscope utilizing multilayer optics in the Schwarzschild configuration. Our prior studies of Schwarzschild multilayer microscopes had been constrained to the development of systems for which high smoothness spherical laser mirrors were available as "off-the-shelf" components. Suitable spherical substrates had been purchased from General Optics of Moorepark, California, and were used for the telescopes flown on October 23, 1987. However, during the development of the MSSTA, we discovered that Phil Baker of Walnut Creek, California could provide substrates of ultra-high smoothness (1 Å rms). This made it possible to consider systems of different diameters and of radii of curvature beyond the limited supply available from other commercial sources.

Prior to the advent of multilayer optics, grazing incidence Wolter x-ray microscope configurations were investigated for applications in x-ray astronomy, where they may be useful for improving the spatial resolution of x-ray telescopes. Hoover et al.⁶ and Shealy and Hoover⁷ theoretically investigated an x-ray microscope with an internally reflecting hyperboloidal mirror followed by an internally reflecting ellipsoidal element for coupling a Wolter Type I telescope optic to a detector. This was considered as a means of increasing the plate scale to allow high resolution images to be achieved with solid state detectors such as CCDs which have inherently lower spatial resolution than photographic emulsions. This system is also restricted to very limited fields of view (a few arc minutes) due to degradation from off-axis aberrations and vignetting effects. Moses et al.⁸ performed a theoretical investigation of an externally reflecting hyperboloid-hyperboloid x-ray microscope optic and found it to yield 1 arc sec resolution over a very limited field of view (1.25 arc minute radius). However, Moses and Davis⁹ report that solar images obtained with this microscope optic produced lower spatial resolution and system throughput than predicted and they attribute these effects to misalignments. Grazing incidence x-ray microscopes for use in combination with telescopes for solar research seem to have severe limitations due to aberrations (strong offense against the Abbé Sine condition) at moderate to large angles off-axis, strong vignetting effects, and severe problems imposed by x-ray scattering. For x-ray sources of small angular subtense, however, Wolter grazing incidence x-ray microscopes offer considerable promise. Laser fusion researchers^{10,11} have used Wolter Type I x-ray microscopes to image imploding targets. A hyperboloidal-ellipsoidal grazing incidence x-ray microscope was fabricated by Franks and Gale.¹² This 22x system was also configured for laser fusion research and operated at a grazing angle of 1 degree. Their experimental results indicated that a spatial resolution of about 1 μm was achieved. Optical aberrations limited the performance. In addition, very low contrast in the image resulted from x-ray scattering effects. Franks and Gale point out that for a grazing incidence system of this

— focal length to achieve spatial resolution of $0.1 \mu\text{m}$ (1000 \AA), the intensity of the scattered radiation must be small at angles no greater than 0.0015 arc sec. This high sensitivity to x-ray scattering taken in conjunction with the fact that it is exceedingly difficult to produce extremely low-scatter grazing incidence mirror systems (and to maintain them sufficiently free from particulate contaminants that x-ray scattering remains low) may be the most serious problem for grazing incidence x-ray microscope optics.

— It is important to note that with normal incidence multilayer optical systems, these major problems can be eliminated. We initially considered the use of single element convex normal incidence multilayer mirrors to magnify the beam from a grazing incidence x-ray telescope and increase the system plate scale. Since the introduction of the normal incidence multilayer optic reduces the system offense against the Abbé Sine condition, it was established that the resolution of such a Spectral Slicing X-Ray Telescope¹³ could be superior to that produced by the grazing incidence optics alone. During the Stanford/MSFC Rocket X-Ray Spectroheliograph flight, the Wolter-Cassegrain component at 44 \AA produced magnified images with noticeably less scattering than that observed in the prime focus of the grazing incidence optic.

— The use of a Schwarzschild x-ray microscope to magnify the image produced by a grazing incidence or multilayer x-ray telescope offers many advantages. First, since the optical system can be folded and utilize both concave and convex mirror systems, the strong offense against the Abbé Sine condition is eliminated. Secondly, systems with improved spectral resolution and very low vignetting can be designed and built. Furthermore, the multilayer optics naturally suppress x-ray scattering. X-ray reflection by multilayer mirrors is the result of an interference process (Bragg diffraction) so that the desired optically reflected intensity is proportional to the square of the amplitude of the diffracted light; whereas, scattered light adds linearly with intensity. Hence, the scattered radiation is naturally suppressed relative to the desired Bragg reflected light. High resolution imaging normal incidence multilayer x-ray microscopes with adequate fields of view and low scatter thus appear to offer great potential.

2. DESIGN AND ANALYSIS OF A SCHWARZSCHILD IMAGING X-RAY MICROSCOPE

— Normal incidence multilayer x-ray optics for use in scanning x-ray microscopes have been investigated by Spiller¹⁴ (using an elliptical mirror) and by Lovas et al.¹⁵ with mirrors of the Schwarzschild configuration for laser fusion research. Trail and Byer¹⁶ developed an x-ray microscope for biological applications. Since it is now established that high quality multilayers mirrors can be produced on concave and convex spherical substrates, and that appropriate bandpass matching to yield high throughput and excellent spatial resolution can be achieved, we have selected the Schwarzschild configuration for our x-ray microscope design. An aplanatic x-ray microscope using two spherical mirrors can be constructed by imposing the Schwarzschild condition¹⁷ on selection of the mirror radii. The Schwarzschild condition can be understood by referring to Figure 1.

— The mirror surfaces S_1 and S_2 are concentric spherical surfaces of radii R_1 and R_2 , respectively. A complete discussion of a ray trace analysis of the Schwarzschild microscope configured for normal incidence multilayer applications was presented by Hoover et al.¹⁸

— The Schwarzschild condition for an aplanatic, two mirror imaging system can be expressed:

$$\frac{R_2}{R_1} = 1.5 - \frac{R_2}{Z_o} \pm \left[1.25 - \frac{R_2}{Z_o} \right]^{1/2}, \quad (1)$$

— where the "+" sign is used in Eq. 1 for magnifications greater than 5, and the "-" sign is used in Eq. 1 for magnifications less than 5.

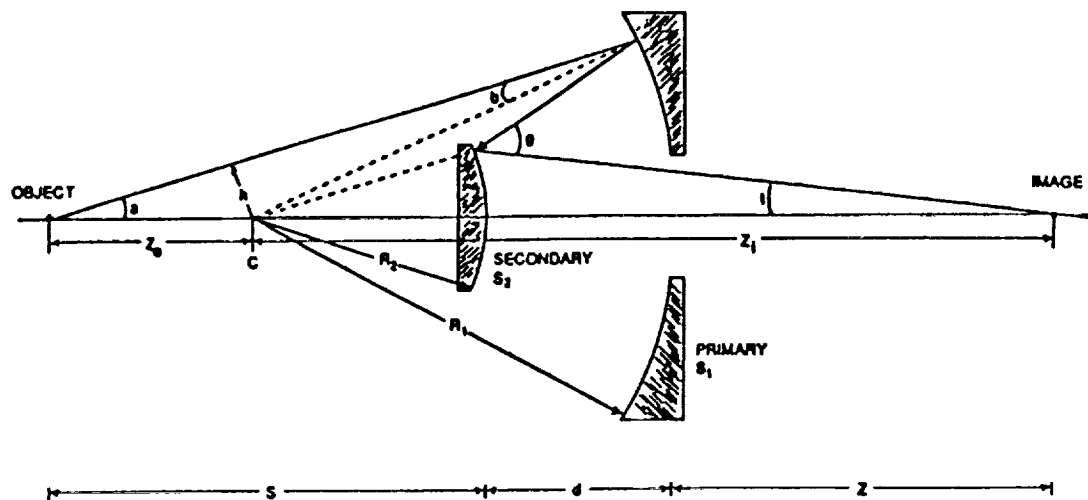


Fig. 1. Schwarzschild configuration for aplanatic normal incidence multilayer x-ray microscope.

The Schwarzschild design equations are summarized¹⁸ and the dependence of the RMS blur circle radius as a function of the object height, image plane location, mirror tilts, and decentration were presented for a 10x microscope with a total length of 1.41 m. Table 1 presents the dependence of the mirror radii of curvature and magnification on system parameters.

TABLE 1

| Schwarzschild Mirror Parameters | | | | | | |
|---------------------------------|------------|------------|----------|----------|----------|----------|
| $M(x)$ | R_1 (cm) | R_2 (cm) | s (cm) | d (cm) | Z (cm) | f (cm) |
| 10 | 31.79 | 10.00 | 18.02 | 21.79 | 48.36 | 7.29 |
| 15 | 29.69 | 10.00 | 18.04 | 19.69 | 91.04 | 7.54 |
| 20 | 28.75 | 10.00 | 18.05 | 18.75 | 131.49 | 7.67 |
| 30 | 27.84 | 10.00 | 18.06 | 17.84 | 213.27 | 7.80 |
| 40 | 27.40 | 10.00 | 18.07 | 17.40 | 296.07 | 7.87 |
| 50 | 27.15 | 10.00 | 18.07 | 17.15 | 376.42 | 7.92 |

The dimensional quantities listed in Table 1 scale in a linear fashion. For example, if R_2 is changed by a factor c to cR_2 , then the new values for the quantities listed in Table 1 except for M will be obtained by multiplying those values given in Table 1 times c .

It now seems practical to construct a multilayer microscope with a secondary radius of curvature equal to 8 cm. Then, the system parameters can be computed and are given in Table 2. Mirror substrates have been ordered for this 20x x-ray microscope. Multilayer coating of these substrates will be optimized for reflection of 125 Å radiation. We present results of the ray trace and diffraction

theory analysis that we have performed for the 20x Schwarzschild microscope which we are currently fabricating.

TABLE 2

| Schwarzschild Microscope System Parameters | |
|--|-----------|
| Magnification | 20x |
| Focal Length | 6.133 cm |
| Primary Mirror | |
| Radius of Curvature | 23.0 cm |
| Outside Diameter | 8.0 cm |
| Hole Diameter | 2.2 cm |
| Secondary Mirror | |
| Radius of Curvature | 8.0 cm |
| Outside Diameter | 2.0 cm |
| Object Distance from Secondary (s) | 14.44 cm |
| Mirror Spacing (d) | 15.0 cm |
| Image Distance from Primary (Z) | 105.19 cm |
| Overall Length ($s + d + Z$) | 134.53 cm |

Figure 2 represents the rms blur circle radius over the image plane $Z_i = 120.016$ cm, which has a minimum rms for an on-axis object point. This figure shows that submicron values of rms blur in the object plane are obtained over an full field of view of 2 mm, which corresponds to an object height of 1 mm. (These object plane rms blur values are obtained by dividing the image plane values given in Figure 2 by the magnification 20x.) Rapid deterioration of the image quality results for object heights greater than 1 mm. We performed a study of the vignetting for the microscope being fabricated. As can be seen in Figure 3, there is almost no vignetting out to an object height of 2 mm. A system with a primary hole diameter of 2 cm exhibits severe loss of energy due to vignetting for object heights greater than 1 mm.

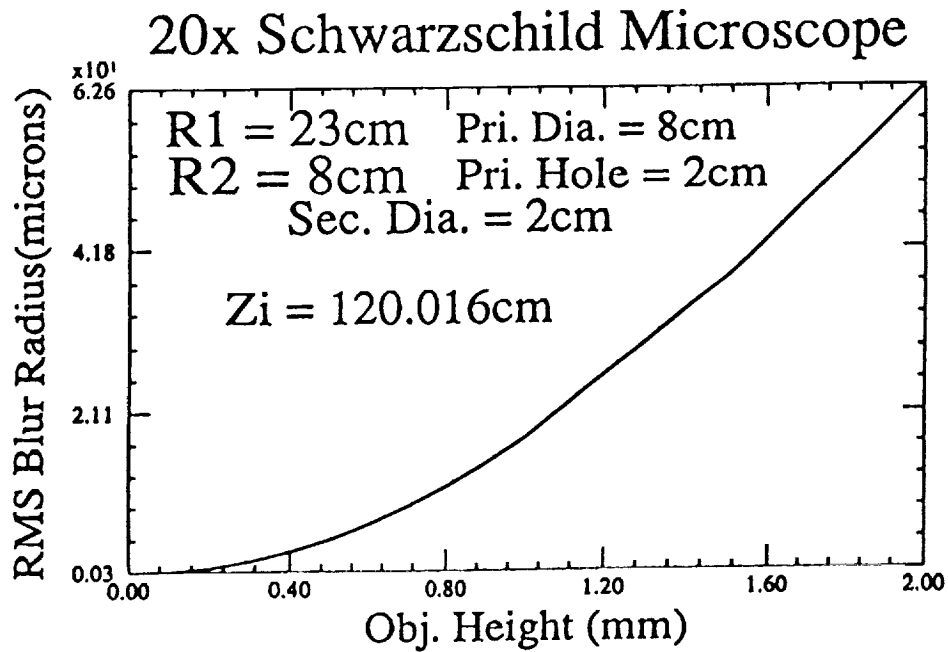


Fig. 2. RMS Blur Radius vs Object Height in the object plane.

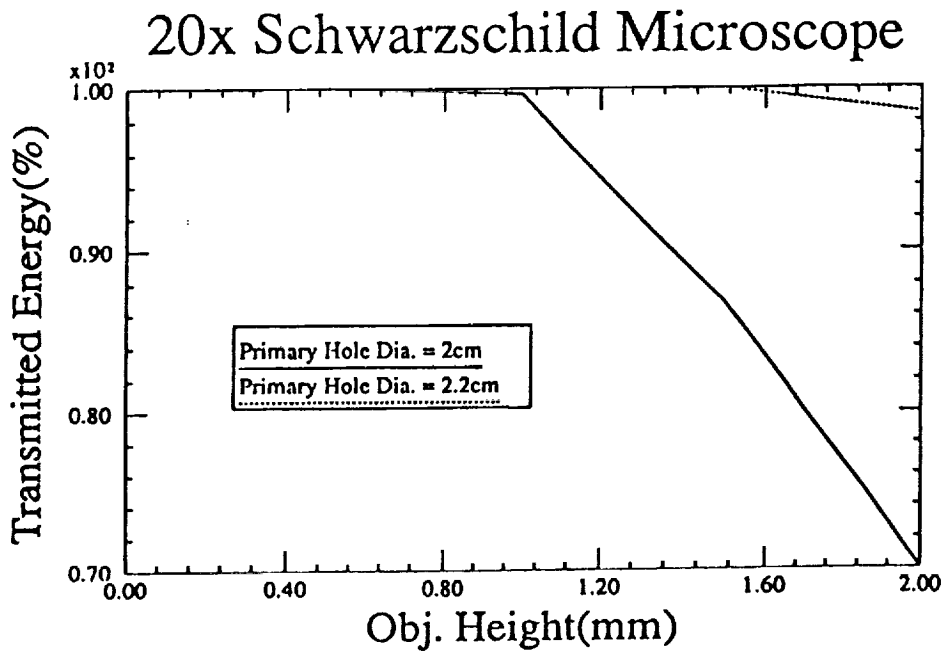


Fig. 3. Transmitted Energy vs Object Height showing effects of vignetting.

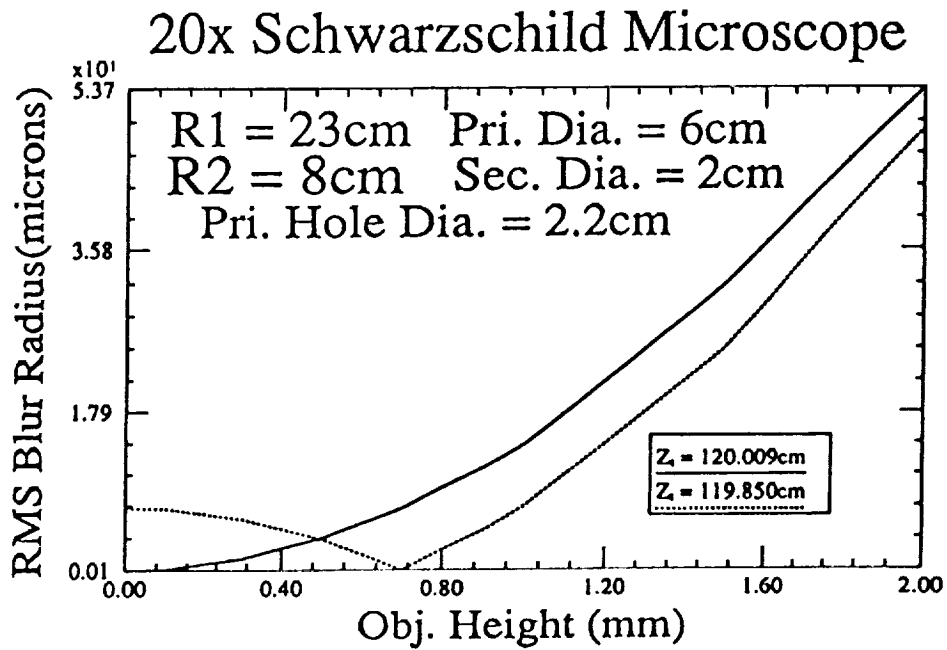


Fig. 4. RMS Blur Radius vs Object Height for defocused image planes.

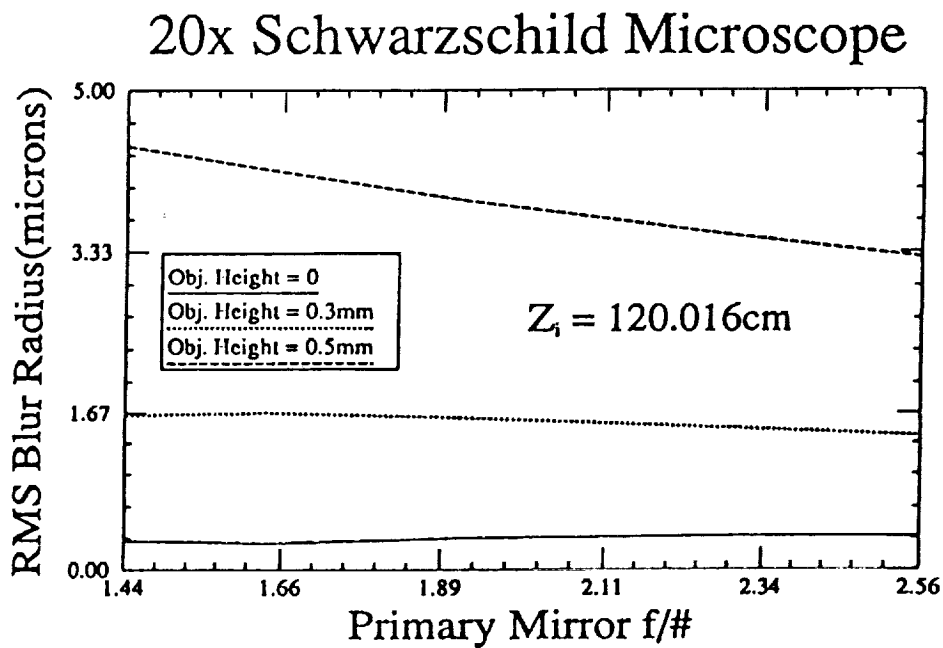


Fig. 5. RMS Blur Radius vs Primary Mirror $f/\#$ for different object heights.

Figure 4 shows the effect of further defocusing the image plane. The RMS blur values in the image plane $Z_i = 119.85$ cm decrease to less than 7 microns for an object height up to 1 mm. This implies that the RMS blur in the object plane should be less than 0.3 microns over a 2 mm full field of view. Figure 5 gives the dependence of RMS blur versus the primary mirror diameter for different object heights where $f/1.44$ corresponds to a 8cm diameter primary, and $f/2.56$ corresponds to a 4.5cm diameter primary. Plots are shown for three different object heights: on-axis, 0.3 mm, and 0.5 mm off-axis. For object points close to the optical axis, the image plane RMS blur does not depend on the primary aperture diameter. For an object height of 0.5 mm, the RMS blur radius decreases as the primary mirror is stopped down.

In order to expand the scale of Fig.2, the RMS blur radius for object heights varying from 0 to 0.5 mm is given in Fig. 6 where $Z_i = 120.19$ cm locates the Gaussian image plane, $Z_i = 120.016$ cm locates the image plane with minimum RMS for an on-axis object, and $Z_i = 119.986$ cm locates the image plane with minimum RMS for an object height of 0.3 mm. Figure 6 shows that RMS blur values less than 0.15 microns in the object plane are achievable over 0.5 mm half field of view.

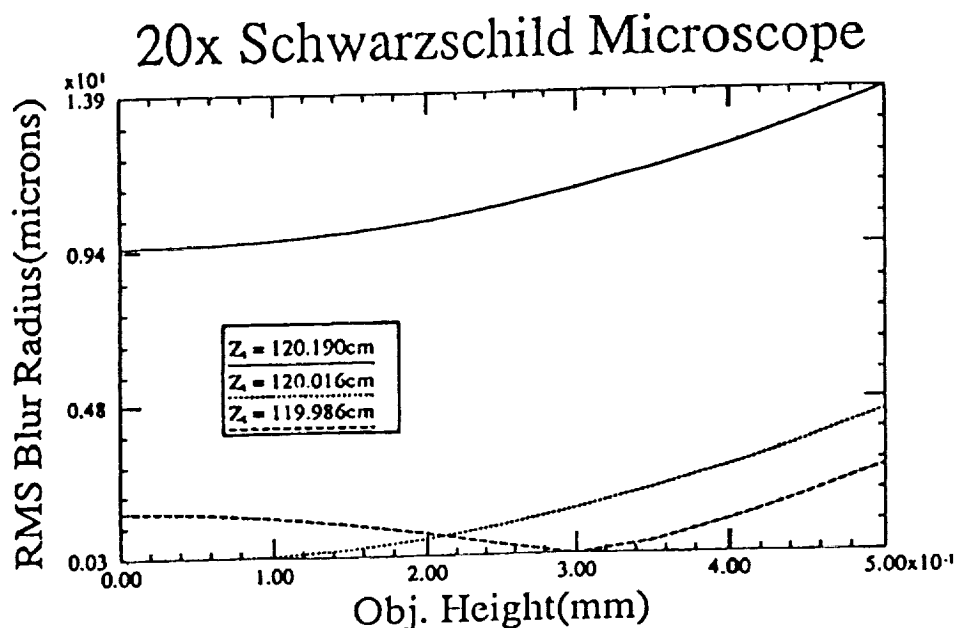


Fig. 6. RMS Blur Radius vs. Object Height over three image planes.

In order to determine the diffraction limited resolution that may be achieved with this microscope, a series of point spread functions over the image plane $Z_i = 120.016$ cm have been evaluated using Fourier diffraction analysis with the General Laser Analysis and Design (GLAD) code, which was developed at Los Alamos National Laboratory and runs on the Cray X/MP supercomputer. Figures 7-10 are three-dimensional point spread functions which show the intensity vs X and Y on the image plane for object heights of 0, 0.5, 0.8, and 1.0 mm. For these calculations, a 450 Å diameter source of 125 Å light was displaced perpendicular to the optical axis to give the corresponding off-axis images. It is interesting to note that the FWHM of the point spread function is 0.78 microns in the image plane up to an object height of 0.5 mm. Since the system magnification is 20x, this implies a spatial resolution of 390 Å in the object plane. This is in fact an upper limit, and higher resolution results may be achieved by using a smaller source to illuminate the microscope optics. For object displacements of 0.8 mm or more, the second and third order diffraction wings increase dramatically and the image quality degrades rapidly.

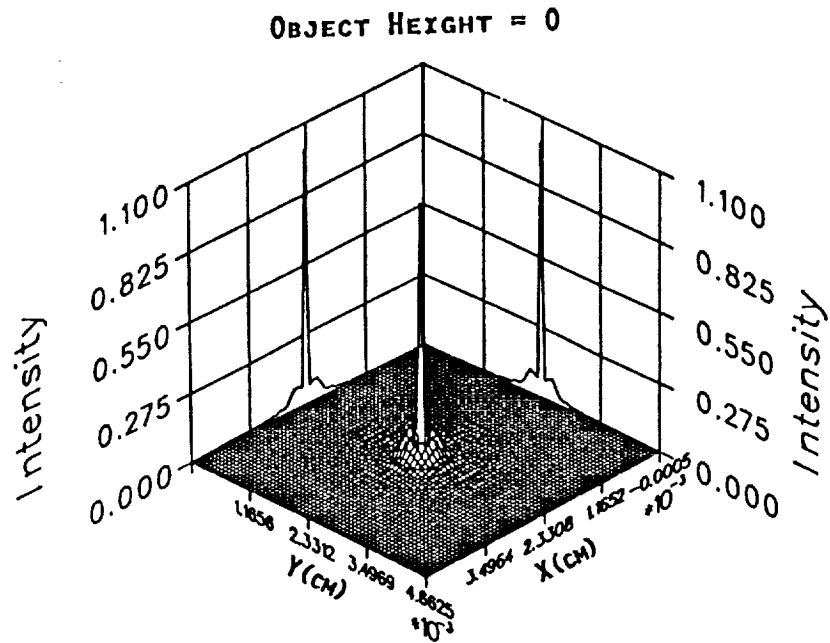


Fig. 7. On-axis three-dimensional point spread function of 20x Schwarzschild X-Ray Microscope using 125 Å radiation.

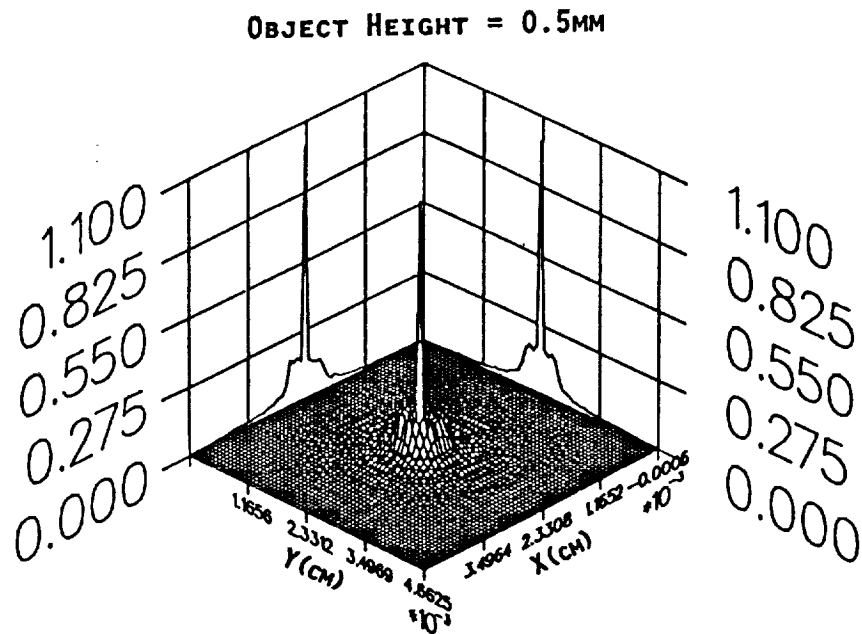


Fig. 8. Three-dimensional point spread function at 0.5 mm off-axis in the object plane. Object plane spatial resolution indicated is 390 Å .

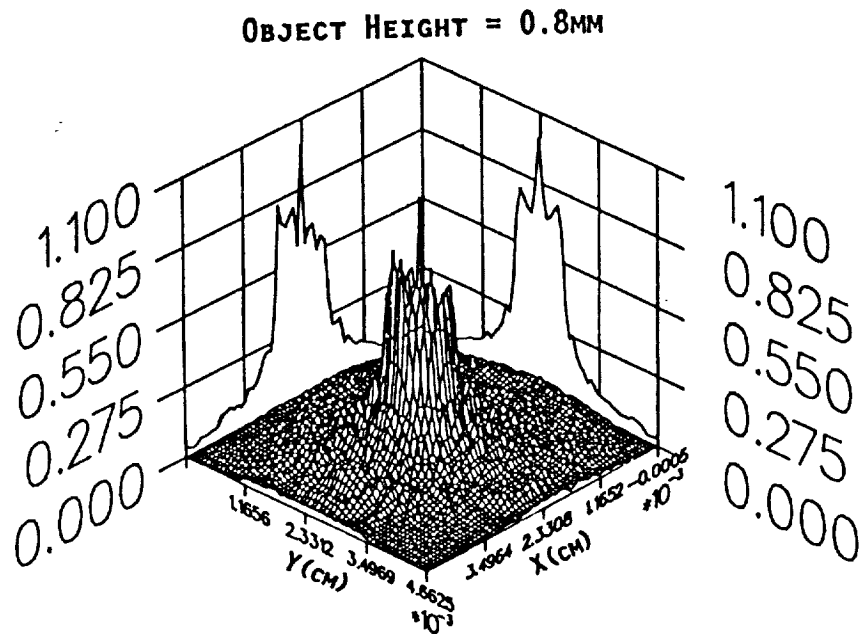


Fig. 9. Three-dimensional point spread function at 0.8 mm off-axis. Spatial resolution in the object plane has degraded to 4600 Å and the central peak is still visible.

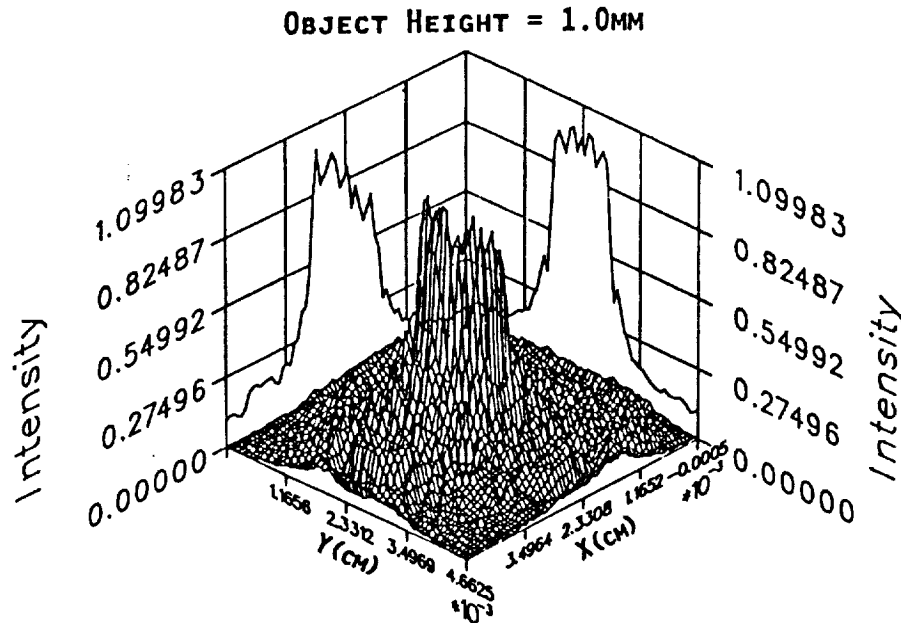


Fig. 10. Three-dimensional point spread function at 1 mm off-axis. Diffraction effects have degraded the resolution to 6600 Å .

These calculations imply that in order to take advantage of this high spatial resolution, photographic emulsions capable of achieving 0.78 micron spatial resolution will be required. This implies the need for films capable of resolving better than 1300 lines per mm over a 20 mm diameter regime. Experimentation is currently ongoing with new improved emulsions and ultra fine-grain developers, and it is believed that these requirements can be met.

3. FABRICATION OF THE 20X SCHWARZSCHILD MICROSCOPE

The 20x Schwarzschild x-ray microscope is being fabricated utilizing much of the technology implemented in the Multi-Spectral Solar Telescope Array (MSSTA) program. Phil Baker of Baker Consulting, Walnut Creek, California is fabricating the mirror substrates from Zerodur. The primary mirrors are concave spheres of 8 cm diameter. They have a radius of curvature of 23 cm and a central hole diameter of 2.2 cm. The convex spherical secondaries are of 2 cm diameter with an 8 cm radius of curvature. The optical surfaces will be polished to 1 \AA rms surface smoothness and surface figure accuracy better than $\frac{\lambda}{10}$ when tested with visible light. The mirror substrates will be coated by one of us (TWB) at the Lawrence Livermore National Laboratory.

We plan to fabricate the microscope tube structures by filament winding methods using AS4-12K graphite fiber with an HBRF55A epoxy resin matrix. Longitudinal fibers will be applied to increase stiffness and to produce microscope tube structures with near zero coefficient of thermal expansion. This is the same technique we have used to fabricate the tube structures for the 12.7 cm diameter telescopes for MSSTA. A completed MSSTA Ritchey-Chrétien telescope is shown in Figure 11.

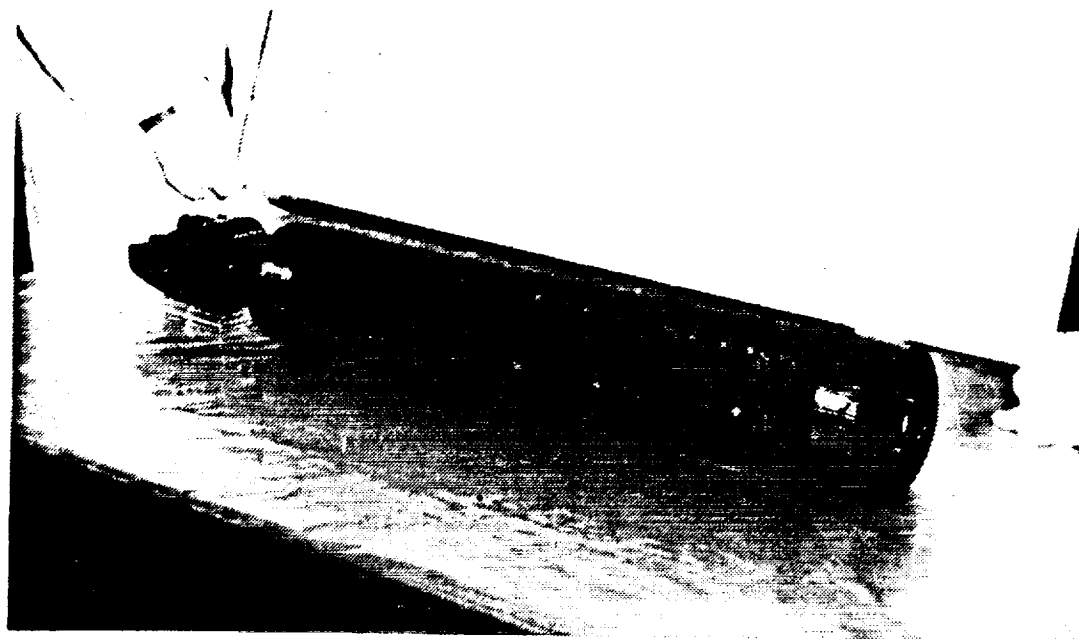


Fig. 11. Graphite epoxy tubes for the Schwarzschild Microscope will be fabricated using similar techniques employed to make this MSSTA 12.7 cm Ritchey-Chrétien telescope.

The camera adapters will accommodate the 35 mm Canon T-70's, which were flown on the Stanford/MSFC Rocket X-Ray Spectroheliograph. Primary data recording will be on 35 mm photographic

film, utilizing the Experimental XUV-100, Experimental XUV-3200, and other emulsions as they become available.

4. CONCLUSIONS

It is now well established that doubly reflecting normal incidence multilayer x-ray optical systems such as we require for the Schwarzschild X-Ray Microscope can be fabricated. Concave and convex hyperboloidal mirror substrates have been fabricated to a surface smoothness of 1 \AA rms for the MSSTA program. Spherical mirror substrates are now being fabricated by Baker Consulting for use in the Schwarzschild x-ray microscope. The high density observed in the photographic images reveals both that excellent soft x-ray/EUV reflectivities are achievable and that accurate matching of the wavelengths of peak reflectivity of the components can be achieved. These results have led us to explore the possibility of producing a high sensitivity, high resolution aplanatic x-ray microscope using normal incidence multilayer mirrors. Our Cassegrain x-ray telescope images and analytical study indicate that soft x-ray/EUV aplanatic imaging multilayer microscopes can be fabricated which will have high throughput and which should be capable of achieving spatial resolution $< 400 \text{ \AA}$.

We have designed several microscopes based on the Schwarzschild configuration and analyzed microscopes of magnifications ranging from 10x to 20x. We have analyzed the rms blur circle radius and the point spread function and determined resolution as a function of object height. We have found the resolution of the 20x system operating at a wavelength of 125 \AA to be less than 400 \AA out to an object height of 0.5 mm giving a 1 mm useful field of view. Mirror substrates are being manufactured for the fabrication of a 20x normal incidence multilayer x-ray microscope with less than 1.5 meter overall length. The initial multilayer coatings to be utilized will be selected to optimize performance at 125 \AA but other coatings will be utilized in accordance with the goals of maximizing throughput and resolution and the nature of the optical systems, objects, or plasma sources for which the microscopes will be used. High resolution aplanatic imaging x-ray microscopes configured from low x-ray scatter normal incidence multilayer optics should be ideal for laser fusion research, biological investigations, and for high spatial resolution astronomical research when used in conjunction with grazing incidence or multilayer x-ray telescope systems.

5. ACKNOWLEDGEMENTS

The Stanford/MSFC Rocket X-Ray Spectroheliograph was funded by NASA Grant NSG 5131 and received its initial support through the Center Director's Discretionary Fund of NASA/MSFC. We also wish to express gratitude to the MSFC CDDF Program for the support provided the current x-ray microscope research.

6. REFERENCES

1. Walker, Arthur B. C., Jr., Lindblom, Joakim F., Hoover, Richard B., and Barbee, Troy W., Jr., "Monochromatic X-Ray and XUV Imaging with Multilayer Optics," *Proc. of International Astronomical Union Colloq. No. 102 on UV and X-Ray Spectroscopy of Astrophysical and Laboratory Plasmas, Beaulieu sur-Mer, France*, eds. F. Bely-Dubau and P. Faucher, in *Journal de Physique-Colloque* 47, C1-175 (1988).
2. Lindblom, Joakim F., Walker, Arthur B. C., Jr., Hoover, Richard B., Barbee, Troy W., Jr., VanPatten Richard A., and Gill, John P., "Soft X-Ray/Extreme Ultraviolet Images of the Solar Atmosphere with Normal Incidence Multilayer Optics," *Proc. SPIE* 982, 316-324 (1988).

3. Hoover, Richard B., Barbee, Troy W., Jr., Lindblom, Joakim F., and Walker, A. B. C., Jr., "Soft X-Ray/XUV Imagery With an Experimental KODAK T-MAX 100 Professional Film," *Kodak Tech Bits*, E. Eggleton, ed., 1-6 (1988).
4. Walker, Arthur B. C., Jr., Barbee, Troy W., Jr., Hoover, Richard B., and Lindblom, Joakim F., "Soft X-Ray Images of the Solar Corona with a Normal-Incidence Cassegrain Multilayer Telescope," *Science* **241**, 1781-1786 (1988).
5. Walker, Arthur B. C., Jr., Lindblom, Joakim F., O'Neal, Ray H., Allen, Maxwell J., Hoover, Richard B., and Barbee, Troy W., Jr., "The Stanford/MSFC Multi-Spectral Solar Telescope Array," *Proc. SPIE* **1160**, (this volume).
6. Hoover, Richard B., Cumings, N. P., Hildner, E., Moore, R. L., and Tandberg-Hanssen, E., "The Extended Range X-Ray Telescope," *NASA TM-86507*, 1-16 (1985).
7. Shealy, David L., and Hoover, Richard B., "Hybrid X-Ray Telescope Systems," *Proc. SPIE* **640**, 28-44 (1986).
8. Moses, J. D., Kreiger, A. S. and Davis, J. M., In *X-Ray Imaging II* (L. Knight and D. Kieth Bowen, eds.), *Proc. SPIE* **691**, 138-147 (1986).
9. Moses, J. Daniel, and Davis, John M., "The Flight Test of a Grazing Incidence Relay Optics Telescope for Solar X-Ray Astronomy Utilizing a Thinned, Back-Illuminated CCD Detector," *Proc. SPIE* **982**, 22-30 (1988).
10. Price, R. H., In *Low Energy X-Ray Diagnostics* (D. T. Attwood, B. L. Henke, eds.), *AIP Conf. Proc.* **75**, American Institute of Physics, New York, 189 (1981).
11. Aoki, S., and Kikuta, S., *Japan J. App. Phys.* **13**, 1385 (1974).
12. Franks, A., and Gale, B., "Grazing Incidence Optics for X-Ray Microscopy," In *X-Ray Microscopy, Proceedings of the International Symposium, Fed. Rep. of Germany, Sept. 14-16, 1983* (G. Schmahl and D. Rudolph, eds.), Springer-Verlag, Berlin, pp. 129-138 (1984).
13. Hoover, Richard B., Shealy, David L., and Chao, Shao-Hua, "Spectral Slicing X-Ray Telescope" *Optical Engineering* **25**, 970-978 (1986).
14. Spiller, E. "A Scanning Soft X-Ray Microscope Using Normal Incidence Mirrors," In *X-Ray Microscopy, Proceedings of the International Symposium, Fed. Rep. of Germany, Sept. 14-16, 1983* (G. Schmahl and D. Rudolph, eds.), Springer-Verlag, Berlin, pp. 226-231 (1984).
15. Lovas, I., Santy, W., Spiller, E., Tibbets, R., and Wilczynski, J., *Proc. SPIE* **316**, 90-97 (1981).
16. Trail, J. A., and Byer, R. L., *Proc. SPIE* **563**, 90-97 (1985).
17. Schwarzschild, K., *Göttingen Mitt* **10**, 2 (1905).
18. Hoover, Richard B., Shealy, David L., Gabardi, David R., Walker, A. B. C., Jr., Lindblom, Joakim F., and Barbee, Troy W., Jr., "Design of an Imaging Microscope for Soft X-Ray Applications," *Proc. SPIE* **984**, 234-246 (1988).

APPENDIX C

"Design and Analysis of a Schwarzschild Imaging Multilayer,
X-Ray Microscope"

David L. Shealy, Richard B. Hoover,
Troy W. Barbee, Jr., and
Arthur B.C. Walker, Jr.

To appear in Optical Engineering, June, 1990

DESIGN AND ANALYSIS OF A SCHWARZSCHILD IMAGING
MULTILAYER X-RAY MICROSCOPE

David L. Shealy

Dept. of Physics, University of Alabama at Birmingham
Birmingham, Alabama 35294

Richard B. Hoover

Space Science Laboratory, NASA Marshall Space Flight Center
Huntsville, Alabama 35812

Troy W. Barbee, Jr.

Lawrence Livermore National Laboratory
Livermore, California 94550

Arthur B. C. Walker, Jr.

Stanford University, Stanford, California 94305

Abstract. Normal incidence multilayer x-ray mirror technology has now advanced to the point that high resolution x-ray microscopes with relatively large fields of view are feasible. High resolution aplanatic imaging x-ray microscopes configured from low x-ray scatter normal incidence multilayer optics should be ideal for laser fusion research, biological investigations, and for astronomical studies when used in conjunction with grazing incidence or multilayer x-ray telescope systems. We have designed several Schwarzschild x-ray microscope optics. Diffraction analysis indicates better than 600 Å spatial resolution in the object plane up to a 0.7 mm field of view can be achieved with 100 Å radiation. We are currently fabricating a 20x normal incidence multilayer x-ray microscope of 1.35 meter overall length. We have also analyzed and designed other microscope systems for use in conjunction with x-ray telescopes. We report on the results of these studies and the x-ray microscope fabrication effort.

Subject terms: x-ray microscopes, multilayers, Schwarzschild objective.

CONTENTS

1. Introduction
2. Design and analysis of a Schwarzschild imaging x-ray microscope
3. Fabrication of the 20x Schwarzschild microscope
4. Conclusions
5. Acknowledgements
6. References

1. INTRODUCTION

High resolution, full-disk solar x-ray images obtained with the Stanford/Marshall Space Flight Center (MSFC) Rocket X-Ray Spectroheliograph clearly demonstrated that both doubly reflecting (Cassegrain) and singly reflecting (Herschelian) multilayer x-ray imaging systems could be successfully implemented.^{1,2} The images obtained with the Cassegrain system at 173 Å and 256 Å show extremely high spatial resolution (~1 arc-sec), and they also reveal that these telescopes have virtually no x-ray scattering. Good full disk solar x-ray images were obtained with a 256 Å Herschelian telescope in exposure times of 0.5 seconds and in 8 second exposures at 44 Å with convex multilayers in the Wolter-Cassegrain configuration.^{1,2} The densities obtained on the photographic emulsions³ in these short exposures clearly indicate that high reflectivities can be achieved with contoured multilayer optics working at normal incidence. The excellent, high density images produced by the 173 Å Cassegrain⁴ conclusively proved that high reflectivity multilayers can be produced on both concave and convex substrates, and that the bandpasses of multilayer mirror components can be accurately matched. Since each multilayer optic reflects effectively in only a relatively narrow bandpass, it is essential that the bandpasses of the primary and secondary elements be accurately matched or very low throughput will result. Recent tests of this Cassegrain telescope, carried out in collaboration with Barry Welsh at the Space Sciences Laboratory of the University of California, Berkeley, and Joakim Lindblom of Stanford University, have confirmed that reflection efficiencies for each telescope mirror exceeded 25% at 173 Å.

The multilayer optics for the 173 Å instrument were made by coating extremely smooth (< 3 Å rms) substrates with Molybdenum/Silicon layers of 36.8 Å and 55.2 Å thickness, respectively.² The normal incidence multilayer Cassegrain telescopes produced full-disk solar soft x-ray/EUV images with almost no x-ray scattering in the 173 Å and 256 Å regions. The solar images have small dark areas which can be clearly seen in close proximity to very bright active regions. Furthermore, low contrast features, such as polar coronal plumes, can be seen in the images. These features would not be so clearly visible if significant x-ray scattering were present. In the 171–175 Å bandpass, the solar emission is dominated by Fe IX and Fe X lines produced by coronal plasma at 0.95–1.3 million degrees Kelvin.

These exciting results with doubly reflecting multilayer telescopes obtained during the flight of the Stanford/MSFC Rocket X-Ray Spectroheliograph led to the development of an entirely new payload, the Multi-Spectral Solar Telescope Array (MSSTA), which is scheduled for launch from the White Sands Missile Range in March, 1990 (see Walker et al.⁵ for a description of this powerful new instrument). These results also encouraged us to continue our efforts to develop an aplanatic imaging x-ray microscope utilizing multilayer optics in the Schwarzschild configuration. Our prior studies of Schwarzschild multilayer microscopes had been constrained to the development of systems for which high smoothness spherical laser mirrors were available as off-the-shelf components. Suitable spherical substrates had been purchased from General Optics of Moorepark, California, and were used for the telescopes flown on October 23, 1987. However, during the development of the MSSTA, we discovered that Phil Baker of Walnut Creek, California could

provide spherical or aspherical substrates of ultra-high smoothness (1 \AA rms). This made it possible to consider systems of different diameters and of radii of curvature beyond the limited supply available from other commercial sources.

Prior to the advent of multilayer optics, grazing incidence Wolter x-ray microscope configurations were investigated for applications in x-ray astronomy, where they may be useful for improving the spatial resolution of x-ray telescopes. Hoover et al.⁶ and Shealy and Hoover⁷ theoretically investigated an x-ray microscope with an internally reflecting hyperboloidal mirror followed by an internally reflecting ellipsoidal element for coupling a Wolter Type I telescope optic to a detector. This was considered as a means of increasing the plate scale to allow high resolution images to be achieved with solid state detectors such as CCDs which have inherently lower spatial resolution than photographic emulsions. This system is restricted to very limited fields of view (a few arc minutes) due to degradation from off-axis aberrations and vignetting effects. Moses et al.⁸ performed a theoretical investigation of an externally reflecting hyperboloid-hyperboloid x-ray microscope optic and found it to yield 1 arc sec resolution over a very limited field of view (1.25 arc minute radius). However, Moses and Davis⁹ report that solar images obtained with this microscope optic produced lower spatial resolution and system throughput than predicted, and they attribute these effects to misalignments. Grazing incidence x-ray microscopes for use in combination with telescopes for solar research seem to have severe limitations due to aberrations (strong offense against the Abbé Sine condition) at moderate to large angles off-axis, strong vignetting effects, and severe problems imposed by x-ray scattering. For x-ray sources of small angular subtense, however,

Wolter grazing incidence x-ray microscopes offer considerable promise. Laser fusion researchers^{10,11} have used Wolter Type I x-ray microscopes to image imploding targets. A hyperboloidal-ellipsoidal grazing incidence x-ray microscope was fabricated by Franks and Gale.¹² This 22x system was also configured for laser fusion research and operated at a grazing angle of 1 degree. Their experimental results indicated that a spatial resolution of about 1 μm was achieved. Optical aberrations limited the performance. In addition, very low contrast in the image resulted from x-ray scattering effects. Franks and Gale point out that for a grazing incidence system of this focal length to achieve spatial resolution of 0.1 μm (1000 \AA), the intensity of the scattered radiation must be small at angles no greater than 0.0015 arc sec. This high sensitivity to x-ray scattering taken in conjunction with the fact that it is exceedingly difficult to produce extremely low-scatter grazing incidence mirror systems (and to maintain them sufficiently free from particulate contaminants that x-ray scattering remains low) may be the most serious problem for grazing incidence x-ray microscope optics.

It is important to note that with normal incidence multilayer optical systems these major problems can be eliminated. We initially considered the use of single element convex normal incidence multilayer mirrors to magnify the beam from a grazing incidence x-ray telescope and increase the system plate scale. Since the introduction of the normal incidence multilayer optic reduces the system offense against the Abbé Sine condition, it was established that the resolution of such a Spectral Slicing X-Ray Telescope¹³ could be superior to that produced by the grazing incidence optics alone. During the Stanford/MSFC Rocket X-Ray Spectroheliograph flight, the Wolter-Cassegrain

component at 44 Å produced magnified images with noticeably less scattering than that observed in the prime focus of the grazing incidence optic.

The use of a Schwarzschild x-ray microscope to magnify the image produced by a grazing incidence or multilayer x-ray telescope offers many advantages. First, since the optical system can be folded and utilize both concave and convex mirror systems, the strong offense against the Abbé Sine condition is eliminated. Secondly, systems with improved spectral resolution and very low vignetting can be designed and built. Furthermore, the multilayer optics naturally suppress x-ray scattering. X-ray reflection by multilayer mirrors is the result of an interference process (Bragg diffraction) so that the desired optically reflected intensity is proportional to the square of the amplitude of the diffracted light; whereas, scattered light adds linearly with intensity. Hence, the scattered radiation is naturally suppressed relative to the desired Bragg reflected light. High resolution imaging normal incidence multilayer x-ray microscopes with adequate fields of view and low scatter thus appear to offer great potential.

2. DESIGN AND ANALYSIS OF A SCHWARZSCHILD IMAGING X-RAY MICROSCOPE

Normal incidence multilayer x-ray optics for use in scanning x-ray microscopes have been investigated by Spiller¹⁴ (using an elliptical mirror) and by Lovas et al.¹⁵ with mirrors of the Schwarzschild configuration for laser fusion research. Trail and Byer¹⁶ developed a scanning x-ray microscope for biological applications. Since it is now established that high quality multilayers mirrors can be produced on concave and convex spherical substrates, and that

appropriate bandpass matching to yield high throughput and excellent spatial resolution can be achieved, we have selected the Schwarzschild configuration for our x-ray microscope design. An aplanatic x-ray microscope using two spherical mirrors can be constructed by imposing the Schwarzschild condition¹⁷ on selection of the mirror radii. The Schwarzschild condition can be understood by referring to Figure 1.

The mirror surfaces S_1 and S_2 are concentric spherical surfaces of radii R_1 and R_2 , respectively. A complete discussion of a ray trace analysis of the Schwarzschild microscope configured for normal incidence multilayer applications was presented by Hoover et al.¹⁸

The Schwarzschild condition for an aplanatic, two mirror imaging system can be expressed:

$$\frac{R_2}{R_1} = 1.5 - \frac{R_2}{Z_0} \pm \left[1.25 - \frac{R_2}{Z_0} \right]^{1/2}, \quad (1)$$

where the "+" sign is used in Eq. 1 for magnifications greater than 5, and the "-" sign is used in Eq. 1 for magnifications less than 5.

The Schwarzschild design equations are summarized¹⁸ and the dependence of the rms blur circle radius as a function of the object height, image plane location, mirror tilts, and decentration were presented for a 10x microscope with a total length of 1.41 m. Table 1 presents the dependence of the mirror radii of curvature and magnification on system parameters. The dimensional quantities listed in Table 1 scale in a linear fashion. For example, if R_2 is changed by a factor c to cR_2 , then the new values for the quantities

listed in Table 1 except for M will be obtained by multiplying those values given in Table 1 times c.

For x-ray microscopy applications, one is interested in resolving small features within a larger field of view of an extended object. Therefore, the diffraction modulation transfer function (MTF)¹⁹⁻²⁰ is an appropriate merit function for evaluating system resolution. The detection system will determine the amount of contrast, that is, value of MTF, in order for a specific microscope to function at a specified resolution. For example, a photo-resist requires a contrast of about 60% in order to record a good image; whereas, the human eye can resolve features with a contrast of about 4%.

In order to evaluate the resolution and field of view capabilities of a Schwarzschild microscope with a wide range of magnifications, the diffraction MTFs and point spread functions (PSFs) have been evaluated over the Gaussian image plane for all microscope systems listed in Table 1 for object heights of 0, 0.35 and 0.5 mm. It is recognized that off axis performance can be improved by defocusing the image plane, but this has not been considered in these calculations. For each system, the numerical aperture (NA) was fixed at 0.1 and 100 Å light was used in all calculations. From Rayleigh's criterion, the diffraction limited resolution of two point sources for these microscopes should be $(= \lambda/2NA)^{21}$ about 0.05 microns without taking into account the effect of the central obscuration¹⁹. The diameter of the primary mirror was adjusted for each magnification to fix the NA at 0.1 for the object distances $(= s + d)$ from Table 1. The diameter of the secondary and the hole in the primary were assumed to be 1.6 cm and 1.8 cm, respectively, for all calculations.

Figures 2 and 3 present the diffraction MTF and PSF for a 5x and 20x Schwarzschild microscope. Comparing Figs. 2 and 3, one notices the scaling of the size of image plane features with magnification. Figure 4 summarizes all these calculations for on axis light where the image plane resolution is plotted as a function of magnification for three values of the MTF. Figure 4 is useful in matching detector resolution capabilities to the required magnification and contrast. By dividing the image plane resolution given in Fig. 4 by the magnification of the microscope, one obtains a measure of object resolution in Fig. 5 for three values of MTF, which is independent of magnification. Thus, improved resolution can be achieved by improving detector sensitivity to contrast. For a detector that can function with $MTF < 20\%$, then the microscope can resolve features smaller than predicted by the Rayleigh criterion, which the reader should recall is based on the separation of two point sources. Whereas, MTF calculations are based on using extended sources. Figure 6 presents the object plane resolution versus object height predicted by calculating the image plane MTF for an off axis object for each microscope given in Table 1, and then, by dividing the image resolution by the magnification. For all magnifications, the object plane resolution were almost equal for a given MTF and object height, but these results were averaged for different magnifications and plotted in Fig. 6. for three object heights of 0, 0.35 mm and 0.5 mm. These results suggest that 600 Å spatial resolution in the object plane can be achieved over an object field of 0.7 mm using a detector that can operate with a 20% MTF.

Assuming film with a grain size of 1 micron is to be used as a detector, then from Figs. 4-6 a magnification of about 20x is required to achieve

resolution less than 0.1 microns over a 0.7 mm field of view. In order to reduce the overall length of the microscope, it is necessary to reduce the radius of curvature of the secondary.

It now seems practical to construct a multilayer microscope with a secondary radius of curvature equal to 8 cm. Then, the system parameters can be computed and are given in Table 2. Mirror substrates have been ordered for this 20x Schwarzschild microscope. Multilayer coating of these substrates will be optimized for reflection of 125 Å radiation. We now present results of the ray trace analysis that we have performed for the 20x Schwarzschild microscope which we are currently fabricating.

Figure 7 represents the rms blur circle radius over the image plane $Z_1 = 120.016$ cm, which has a minimum rms for an on-axis object point. This figure shows that submicron values of rms blur in the object plane are obtained over an full field of view of 2 mm, which corresponds to an object height of 1 mm. (These object plane rms blur values are obtained by dividing the image plane values given in Figure 7 by the magnification 20x.) Rapid deterioration of the image quality results for object heights greater than 1 mm. We performed a study of the vignetting for the microscope being fabricated. As can be seen in Figure 8, there is almost no vignetting out to an object height of 2 mm. A system with a primary hole diameter of 2 cm exhibits severe loss of energy due to vignetting for object heights greater than 1 mm.

Figure 9 shows the effect of further defocusing the image plane. The rms blur values in the image plane $Z_1 = 119.85$ cm decrease to less than 7 microns for an object height up to 1 mm. This implies that the rms blur in the object plane should be less than 0.3 microns over a 2 mm full field of

view. Figure 10 gives the dependence of rms blur versus the primary mirror diameter for different object heights where $f/1.44$ corresponds to a 8 cm diameter primary, and $f/2.56$ corresponds to a 4.5cm diameter primary. Plots are shown for three different object heights: on-axis, 0.3 mm, and 0.5 mm off-axis. For object points close to the optical axis, the image plane rms blur does not depend on the primary aperture diameter. For an object height of 0.5 mm, the rms blur radius decreases as the primary mirror is stopped down.

In order to expand the scale of Figure 7, the rms blur radius for object heights varying from 0 to 0.5 mm is given in Figure 11 where $Z_i = 120.19$ cm locates the Gaussian image plane, $Z_i = 120.016$ cm locates the image plane with minimum rms for an on-axis object, and $Z_i = 119.986$ cm locates the image plane with minimum rms for an object height of 0.3 mm. Figure 11 shows that rms blur values less than 0.15 microns in the object plane are achievable over 0.5 mm half field of view.

These calculations imply that in order to take advantage of this high spatial resolution, photographic emulsions capable of achieving submicron spatial resolution will be required. This implies the need for films capable of resolving better than 1300 lines per mm over a 20 mm diameter regime. Experimentation is currently ongoing with new improved emulsions and ultra fine-grain developers, and it is believed that these requirements can be met.

3. FABRICATION OF THE 20X SCHWARZSCHILD MICROSCOPE

The 20x Schwarzschild x-ray microscope is being fabricated utilizing much of the technology implemented by the Multi-Spectral Solar Telescope Array (MSSTA) program. Phil Baker of Baker Consulting, Walnut Creek, California

is fabricating the mirror substrates from Zerodur. The primary mirrors are concave spheres of 8 cm diameter. They have a radius of curvature of 23 cm and a central hole diameter of 2.2 cm. The convex spherical secondaries are of 2 cm diameter with an 8 cm radius of curvature. The optical surfaces will be polished to 2-3 Å rms surface smoothness and surface figure accuracy better than $\frac{\lambda}{10}$ when tested with visible light. The mirror substrates will be coated by one of us (TWB) at the Lawrence Livermore National Laboratory.

We plan to fabricate the microscope tube structures by filament winding methods using AS4-12K graphite fiber with an HBRF55A epoxy resin matrix. Longitudinal fibers will be applied to increase stiffness and to produce microscope tube structures with near zero coefficient of thermal expansion. This is the same technique we have used to fabricate the tube structures for the 12.7 cm diameter telescopes for MSSTA. The camera adapters will accommodate either 35 mm Canon T-70's, which were flown on the Stanford/MSFC Rocket X-Ray Spectroheliograph or 70 mm Pentax 645's, which will be flown on MSSTA. Primary data recording will be on experimental XUV 100 and other x-ray/EUV sensitive emulsions.

4. CONCLUSIONS

It is now well established that doubly reflecting normal incidence multilayer x-ray optical systems such as we require for the Schwarzschild X-Ray Microscope can be fabricated. Concave and convex hyperboloidal mirror substrates have been fabricated to a surface smoothness of 2-3 Å rms for the MSSTA program. The high density observed in the solar rocket images reveals both that excellent soft x-ray/EUV reflectivities are achievable and that

accurate matching of the wavelengths of peak reflectivity of the components can be achieved. These results have led us to explore the possibility of producing a high sensitivity, high resolution aplanatic x-ray microscope using normal incidence multilayer mirrors. Our Cassegrain x-ray telescope images and analytical study indicates that soft x-ray/EUV aplanatic imaging multilayer microscopes can be fabricated which will have high throughput and which should be capable of achieving spatial resolution less than 600 Å .

We have designed several microscopes based on the Schwarzschild configuration and analyzed microscopes of magnifications ranging from 2x to 50x. We have analyzed the rms blur circle radius, the MTF, and the point spread function and determined resolution as a function of object height. We have found the resolution of the 20x system operating at a wavelength of 100 Å to be less than 600 Å for an object height of 0.35 mm giving a 0.7 mm useful field of view. Mirror substrates are being manufactured for the fabrication of a 20x normal incidence multilayer x-ray microscope with less than 1.5 meter overall length. The initial multilayer coatings to be utilized will be selected to optimize performance at 125 Å but other coatings will be utilized in accordance with the goals of maximizing throughput and resolution and the nature of the optical systems, objects, or plasma sources for which the microscopes will be used. High resolution aplanatic imaging x-ray microscopes configured from low x-ray scatter normal incidence multilayer optics should be ideal for laser fusion research, biological investigations, and for high spatial resolution astronomical research when used in conjunction with grazing incidence or multilayer x-ray telescope systems.

5. ACKNOWLEDGEMENTS

The Stanford/MSFC Rocket X-Ray Spectroheliograph was funded by NASA Grant NSG 5131 and received its initial support through the Center Director's Discretionary Fund of NASA/MSFC, which is provider of some support for the current x-ray microscope research. We also wish to express gratitude to Phil Baker for his effort in mirror fabrication and to Alabama Supercomputer Network for providing time on the Cray X/MP-24 for some diffraction calculations.

6. REFERENCES

1. A. B. C. Walker, Jr., J. F. Lindblom, R. B. Hoover, and T. Barbee, Jr. "Monochromatic X-Ray and XUV Imaging with Multilayer Optics," in Journal de Physique-Colloque, F. Bely-Dubau and P. Faucher, eds., Proc. of International Astronomical Union Colloq. No. 102 on UV and X-Ray Spectroscopy of Astrophysical and Laboratory Plasmas **47**, C1-175 (1988).
2. J. F. Lindblom, A. B. C. Walker, Jr., R. B. Hoover, T. W. Barbee, Jr., R. A. VanPatten and J. P. Gill, "Soft X-Ray/Extreme Ultraviolet Images of the Solar Atmosphere with Normal Incidence Multilayer Optics," Proc. SPIE **982**, 316-324 (1988).
3. R. B. Hoover, T. W. Barbee, Jr., J. F. Lindblom, and A. B. C. Walker, Jr., "Soft X-Ray/XUV Imagery With an Experimental KODAK T-MAX 100 Professional Film," Kodak Tech Bits, E. Eggleton, ed., pp. 1-6 (1988).

4. A. B. C. Walker, Jr., T. W. Barbee, Jr., R. B. Hoover, and J. F. Lindblom, "Soft X-Ray Images of the Solar Corona with a Normal-Incidence Cassegrain Multilayer Telescope," *Science* **241**, 1781-1786 (1988).
5. A. B. C. Walker, Jr., J. F. Lindblom, R. H. O'Neal, M. J. Allen, T. W. Barbee, Jr., and R. B. Hoover, "The Stanford/MSFC Multi-Spectral Solar Telescope Array," *Proc. SPIE* **1160**, 131-144 (1989).
6. R. B. Hoover, N. P. Cumings, E. Hildner, R. L. Moore, and E. Tandberg-Hanssen, "The Extended Range X-Ray Telescope," NASA TM-86507, 1-16 (1985).
7. D. L. Shealy, and R. B. Hoover, "Hybrid X-Ray Telescope Systems," *Proc. SPIE* **640**, 28-44 (1986).
8. J. D. Moses, A. S. Kreiger, and J. M. Davis, in X-Ray Imaging II, L. Knight and D. Kieth Bowen, eds., *Proc. SPIE* **691**, 138-147 (1986).
9. J. D. Moses, and J. M. Davis, "The Flight Test of a Grazing Incidence Relay Optics Telescope for Solar X-Ray Astronomy Utilizing a Thinned, Back-Illuminated CCD Detector," *Proc. SPIE* **982**, 22-30 (1988).
10. R. H. Price, in Low Energy X-Ray Diagnostics, D. T. Attwood, B. L. Henke, eds., AIP Conf. Proc. **75**, American Institute of Physics, New York, 189 (1981).
11. S. Aoki and S. Kikuta, *Japan J. App. Phys.* **13**, 1385 (1974).
12. A. Franks and B. Gale, "Grazing Incidence Optics for X-Ray Microscopy," in X-Ray Microscopy, Proceedings of the International Symposium, Fed. Rep. of Germany, Sept. 14-16, 1983, G. Schmahl and D. Rudolph, eds., Springer-Verlag, Berlin, pp. 129-138 (1984).

13. R. B. Hoover, D. L. Shealy, and S. H. Chao, "Spectral Slicing X-Ray Telescope," *Optical Engineering* **25**, 970-978 (1986).
14. E. Spiller, "A Scanning Soft X-Ray Microscope Using Normal Incidence Mirrors," in X-Ray Microscopy, Proceedings of the International Symposium, Fed. Rep. of Germany, Sept. 14-16, 1983, G. Schmahl and D. Rudolph, eds., Springer-Verlag, Berlin, pp. 226-231 (1984).
15. I. Lovas, W. Santy, E. Spiller, R. Tibbets, and J. Wilczynski, J., Proc. SPIE **316**, 90-97 (1981).
16. J. A. Trail, and R. L. Byer, Proc. SPIE **563**, 90-97 (1985).
17. K. Schwarzschild, *Gottingen Mitt* **10**, 2 (1905).
18. R. B. Hoover, D. L. Shealy, D. L. Gabardi, A. B. C. Walker, Jr., J. F. Lindblom, and Troy W. Barbee, Jr., "Design of an Imaging Microscope for Soft X-Ray Applications," Proc. SPIE **984**, 234-246 (1988).
19. W. J. Smith, Modern Optical Engineering, pp. 308-325, McGraw-Hill, New York (1966).
20. C. S. Williams and O. A. Becklund, Introduction to the Optical Transfer Function, John Wiley & Sons, New York (1989).
21. F. A. Jenkins and H. E. White, Fundamentals of Optics, Fourth Edition, pp. 332-333, McGraw-Hill, St. Louis (1976).

Figure Captions

1. Schwarzschild configuration for aplanatic normal incidence multilayer x-ray microscope.
2. Diffraction MTF and point spread function for a 5x microscope.
3. Diffraction MTF and point spread function for a 20x microscope.
4. Gaussian image plane resolution versus magnification for 100 Å light.
5. Object plane resolution versus magnification for 100 Å light.
6. Object plane resolution versus object height for 100 Å light.
7. RMS blur radius vs object height in the object plane.
8. Transmitted energy vs object height showing effects of vignetting.
7. On-axis three-dimensional point spread function of 20x Schwarzschild X-Ray Microscope using 125 Å radiation.
8. Three-dimensional point spread function at 0.5 mm off-axis in the object plane. Object plane spatial resolution indicated is 390 Å .
9. RMS blur radius vs object height for defocused image planes.
10. RMS blur radius vs primary mirror f/# for different object heights.
11. RMS blur radius vs. object height over three image planes.

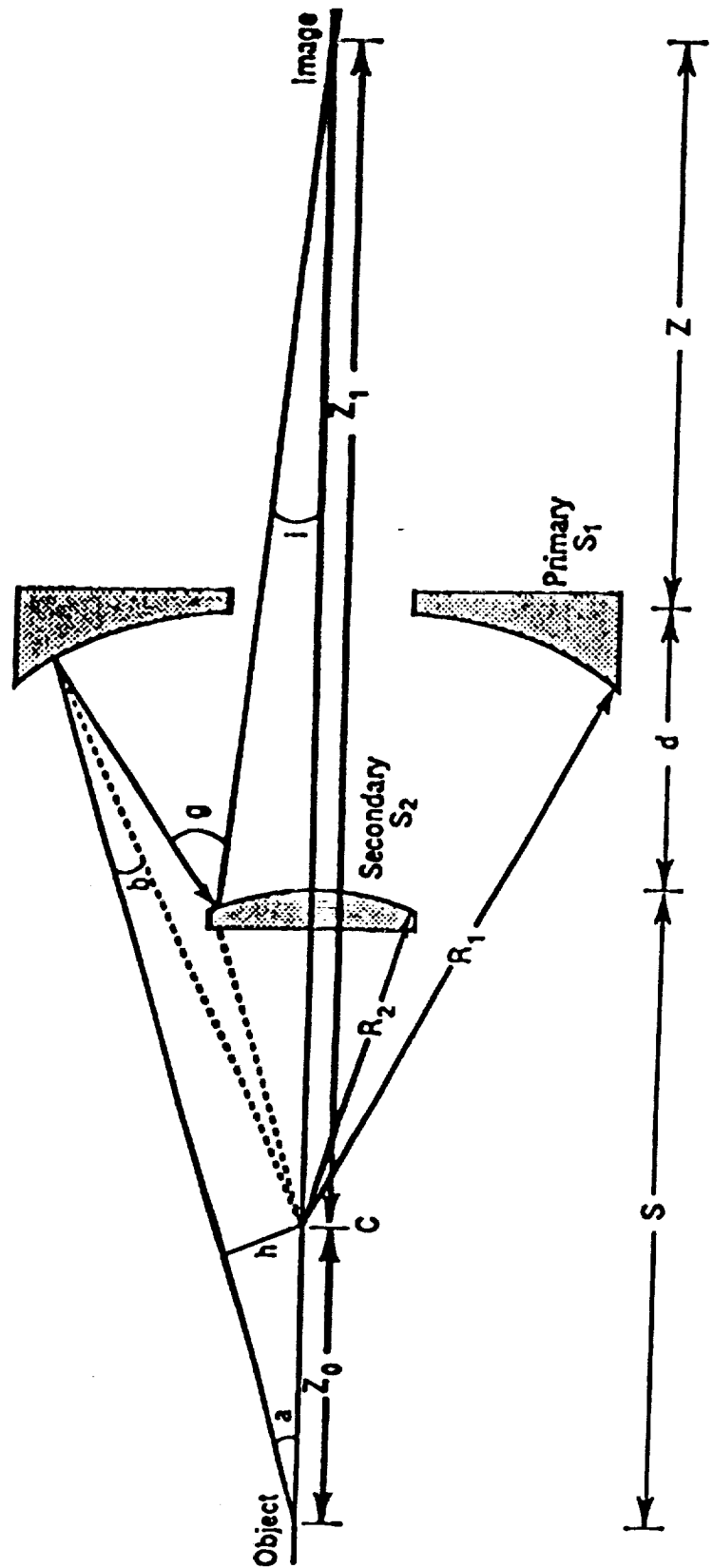


Fig. 1. Schwarzschild configuration for aplanatic normal incidence multilayer x-ray microscope.

SCHWARZSCHILD MICROSCOPE (5X)

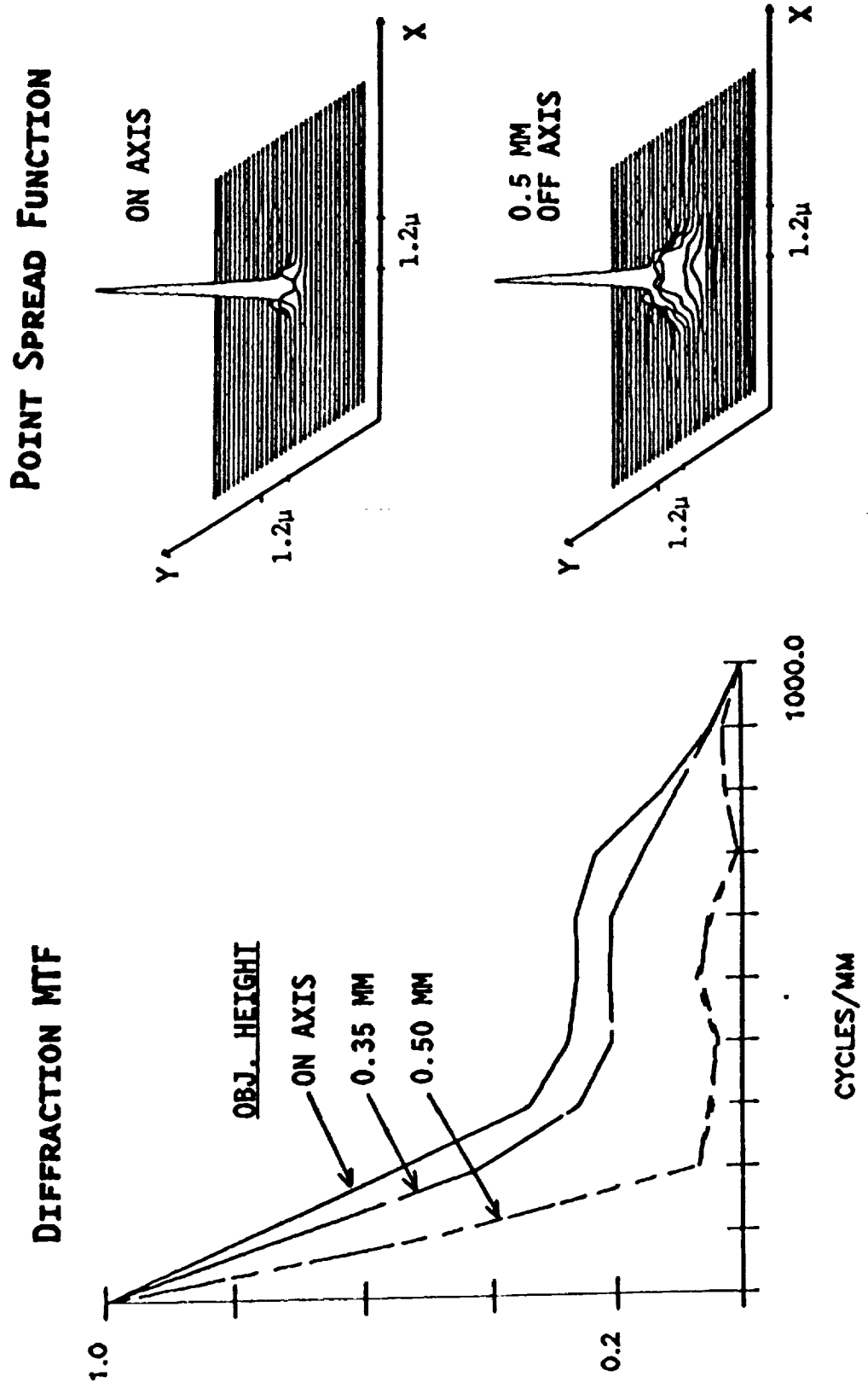
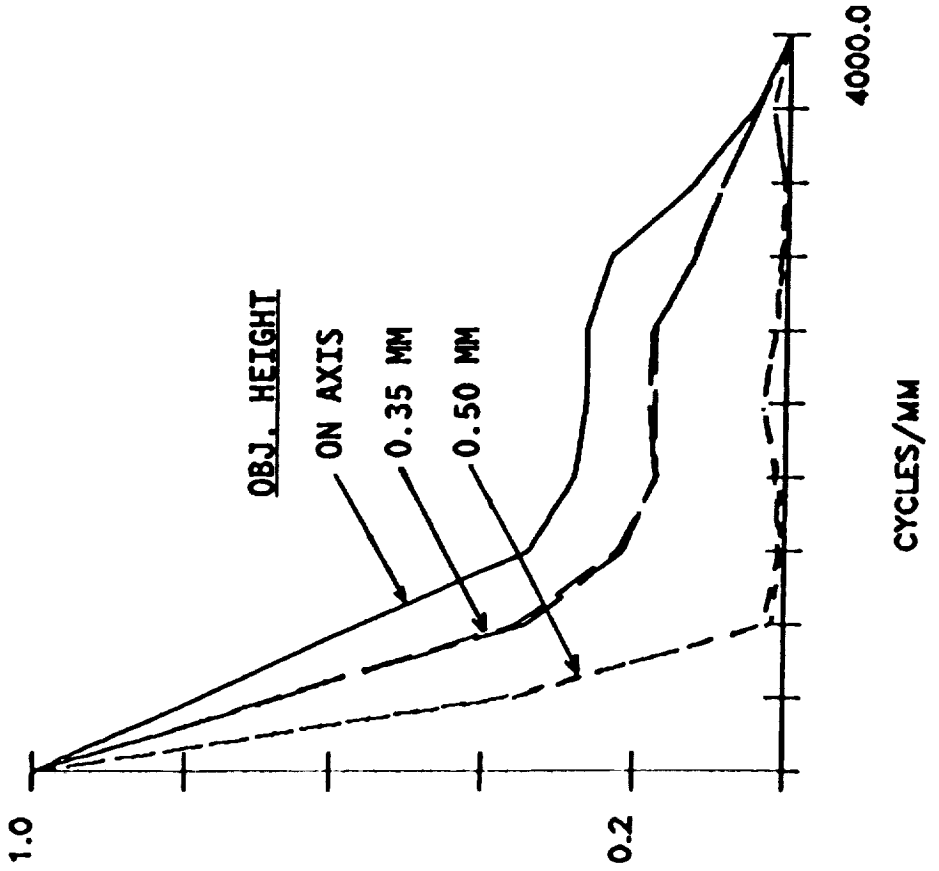


Fig. 2. Diffraction MTF and point spread function for a 5x microscope.

SCHWARZSCHILD MICROSCOPE (20X)

DIFFRACTION MTF



POINT SPREAD FUNCTION

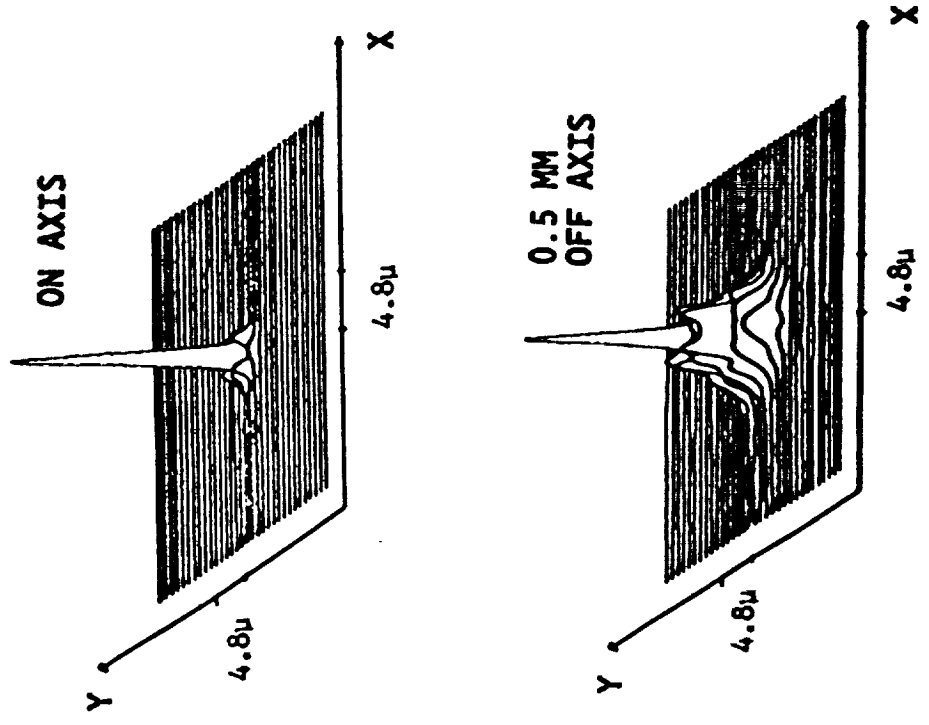


Fig. 3. Diffraction MTF and point spread function for a 20x microscope.

Schwarzschild Microscope

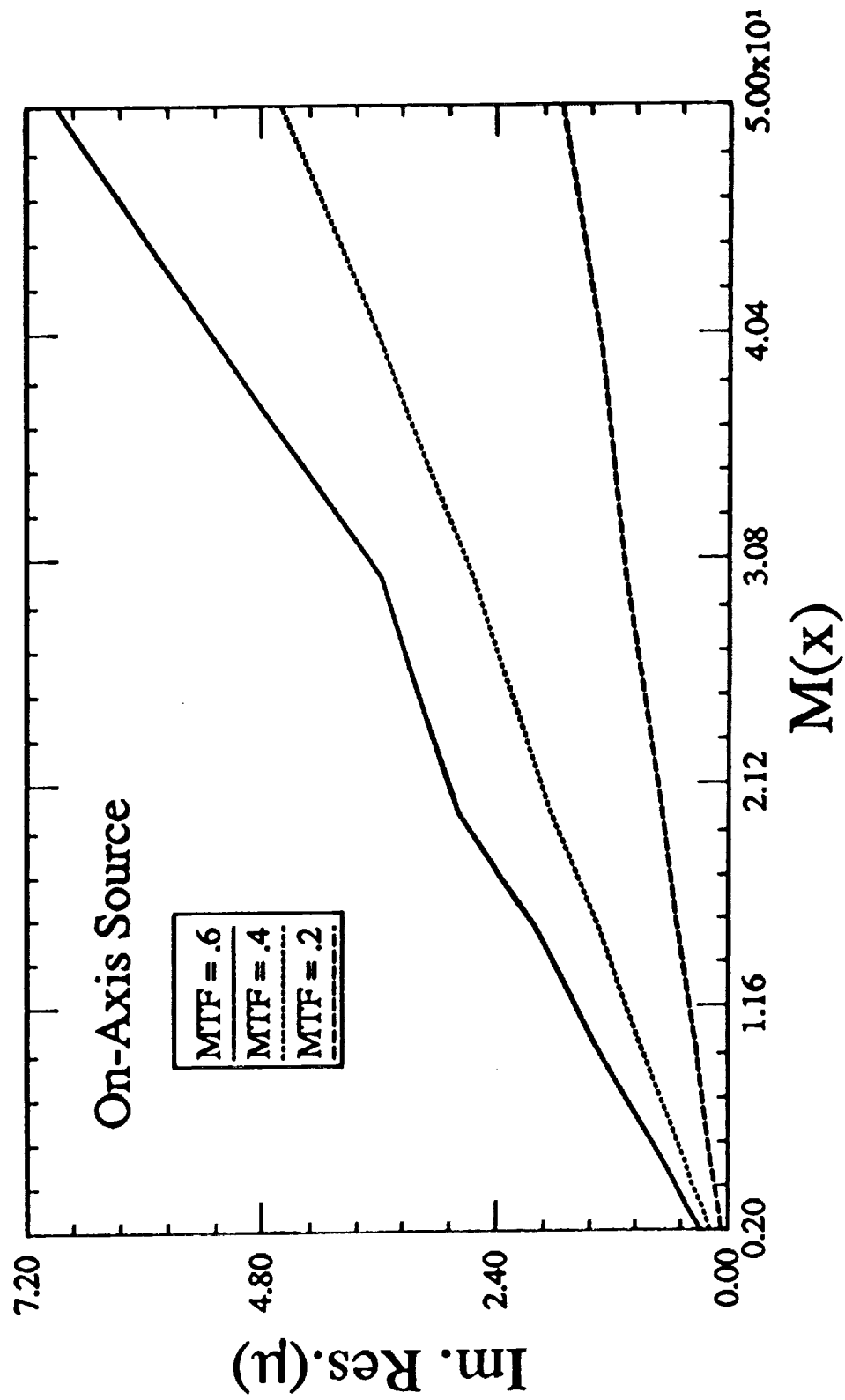


Fig. 4. Gaussian image plane resolution versus magnification for 100 Å light.

Schwarzschild Microscope

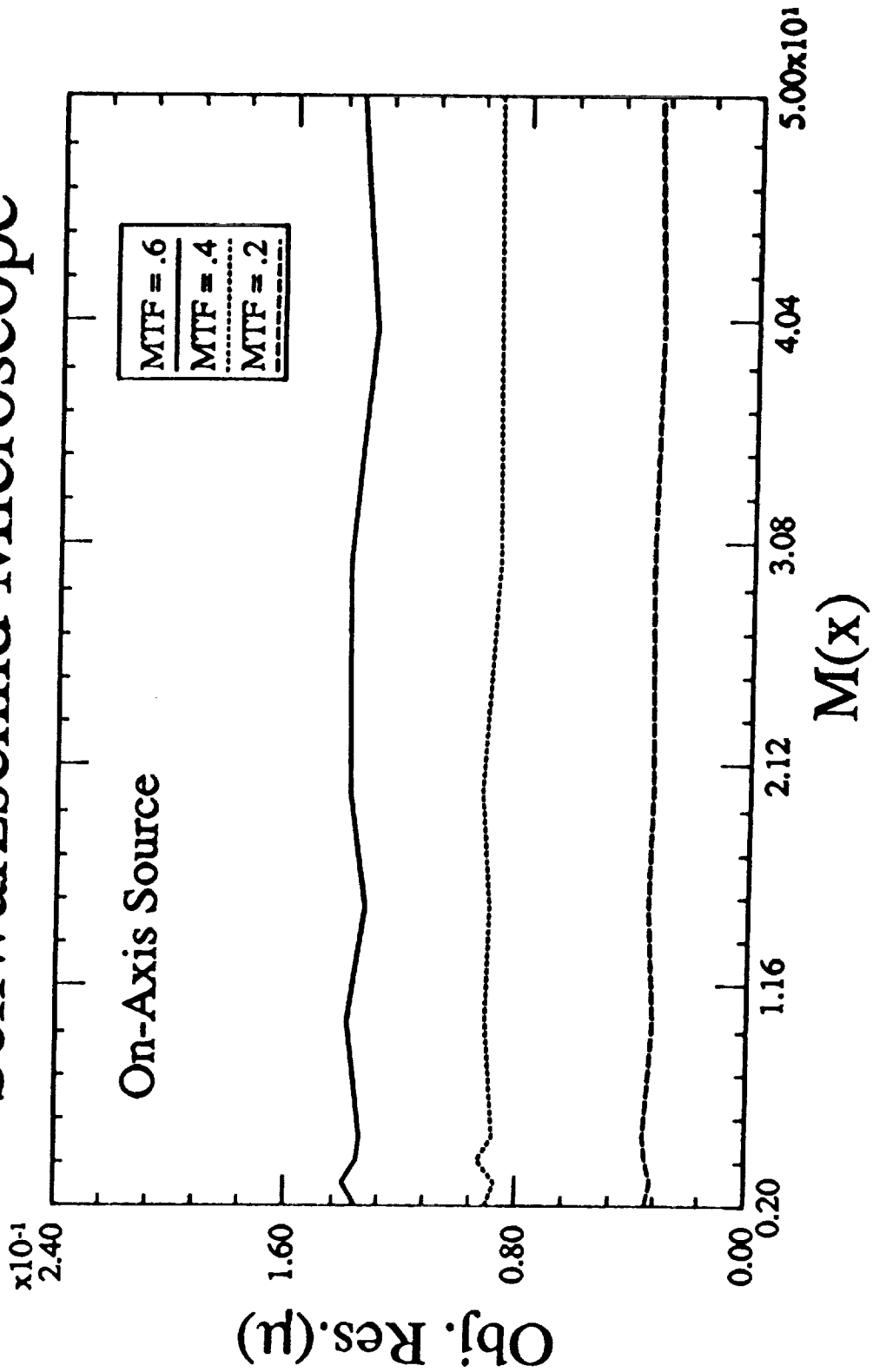


Fig. 5. Object plane resolution versus magnification for 100 Å light.

Schwarzschild Microscope

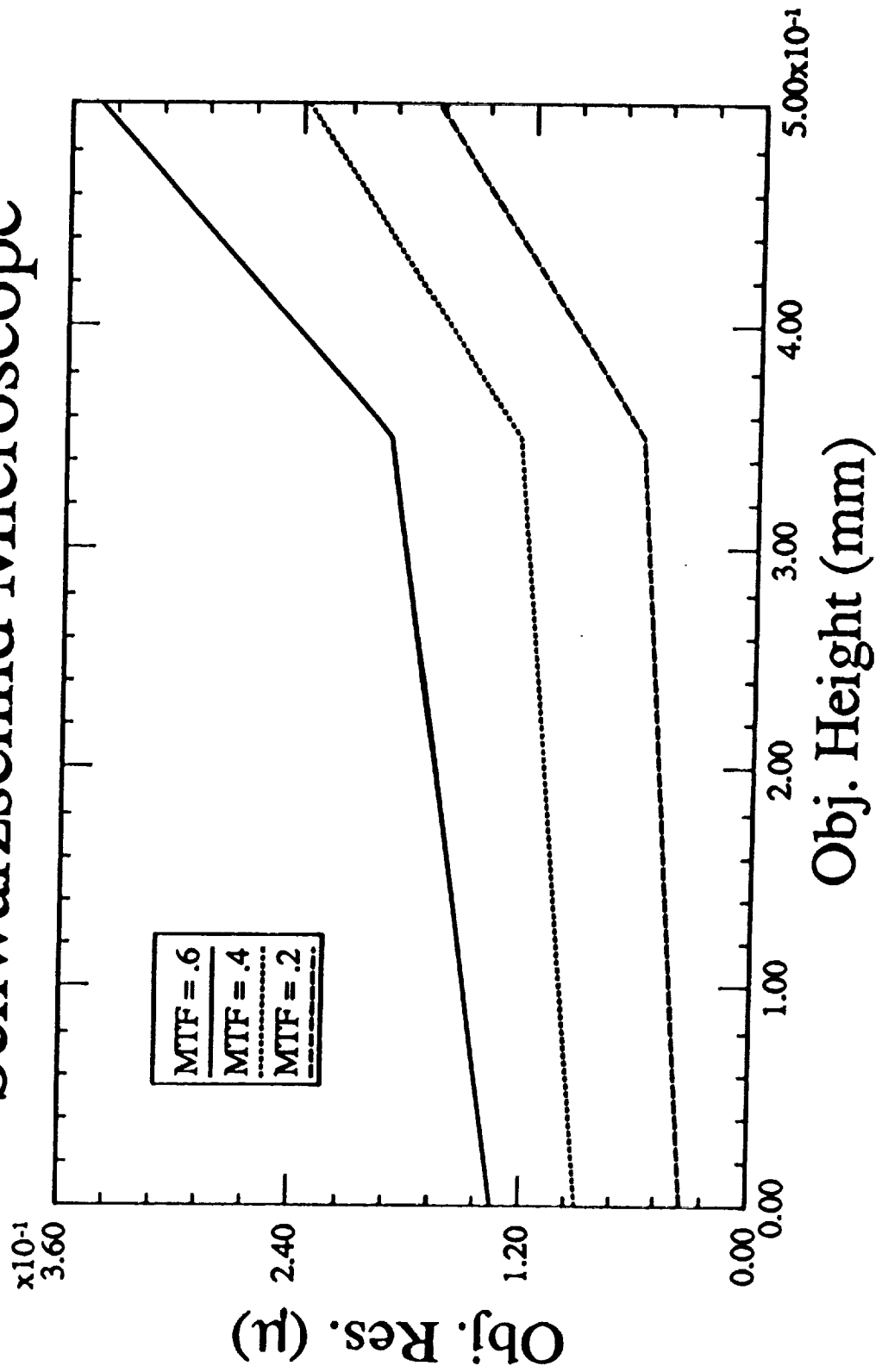


Fig. 6. Object plane resolution versus object height for 100 Å light.

20x Schwarzschild Microscope

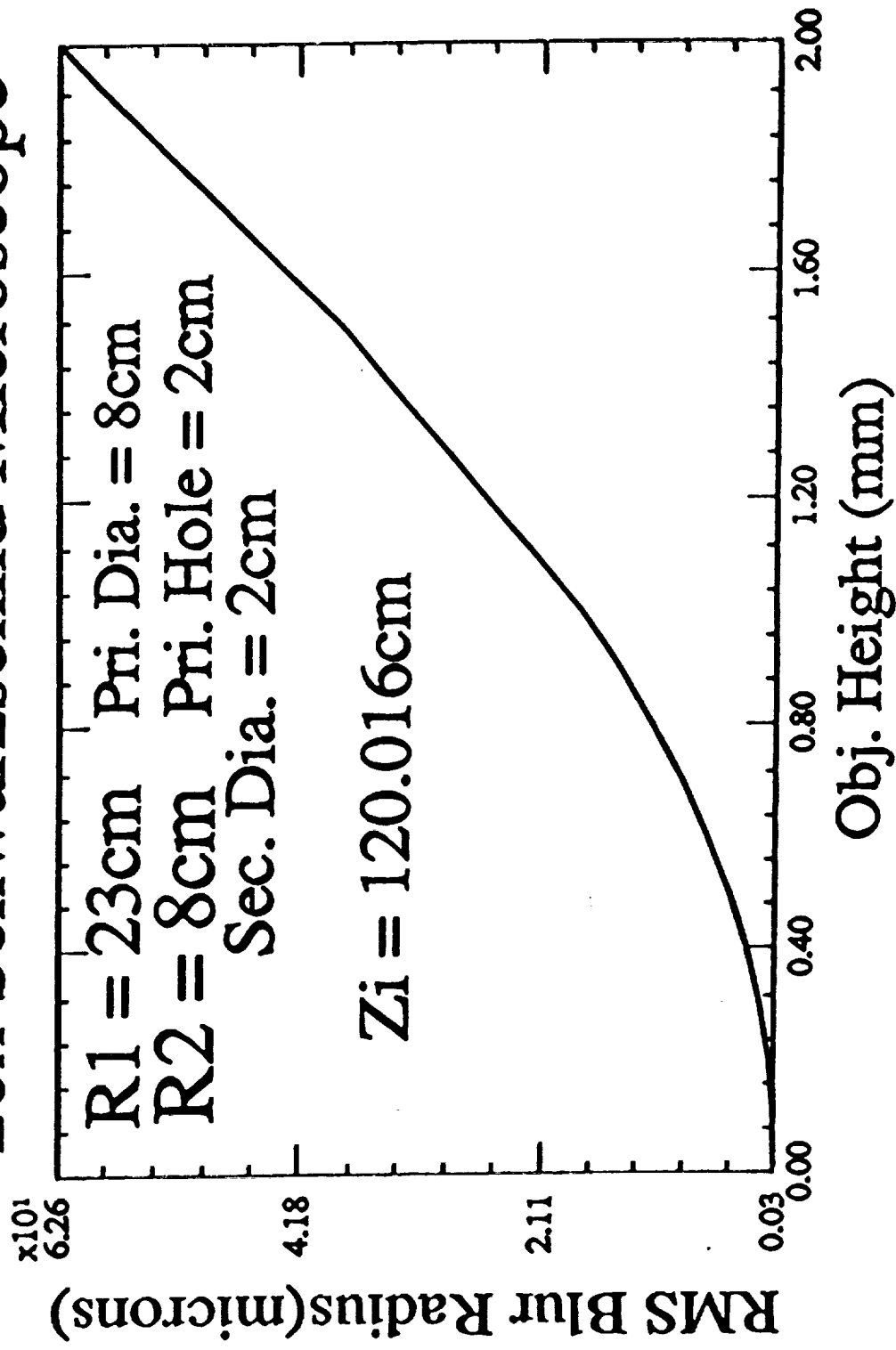


Fig. 7. RMS blur radius vs object height in the object plane.

20x Schwarzschild Microscope

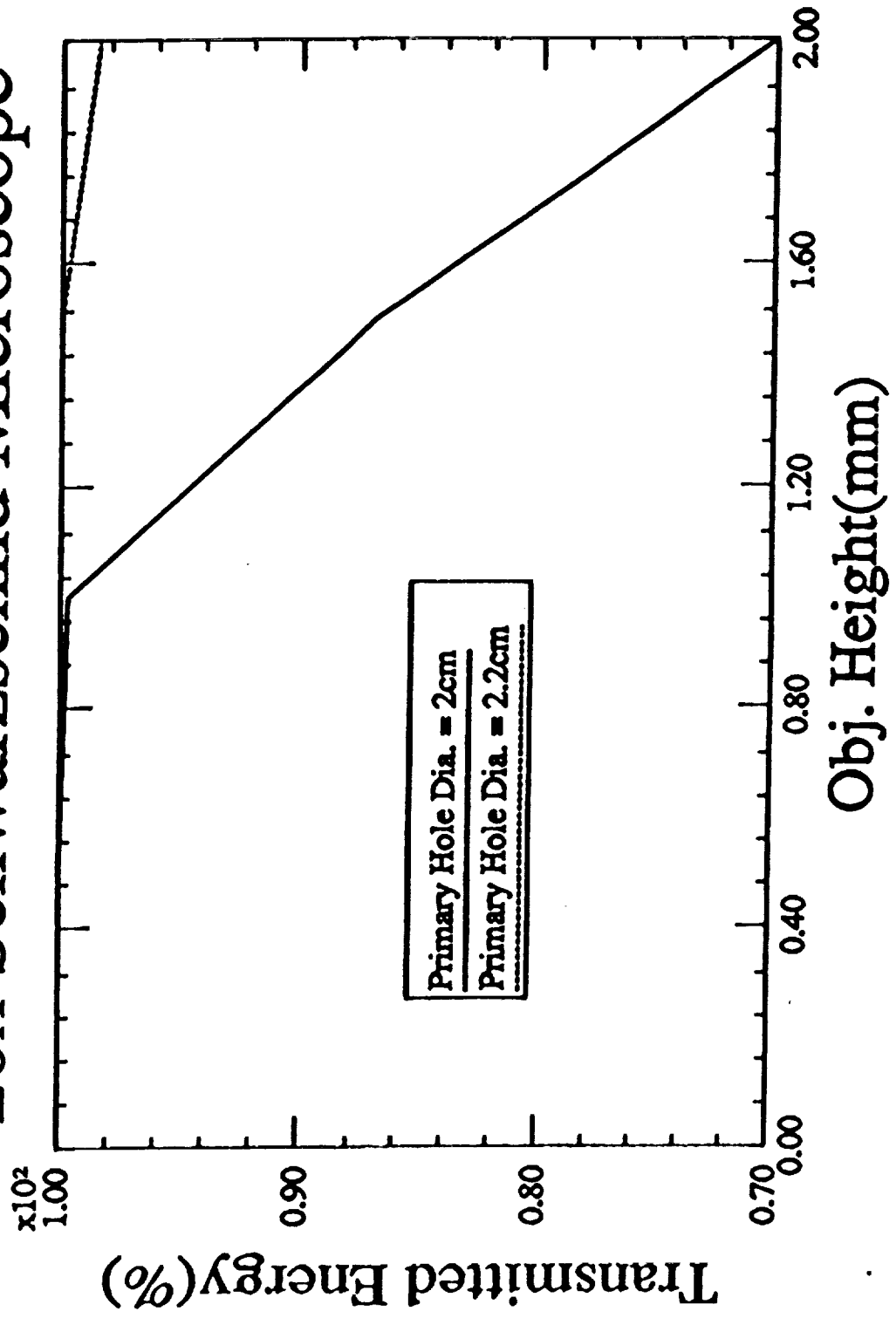


Fig. 8. Transmitted energy vs object height showing effects of vignetting.

20x Schwarzschild Microscope

R1 = 23cm Pri. Dia. = 6cm
R2 = 8cm Sec. Dia. = 2cm
Pri. Hole Dia. = 2.2cm

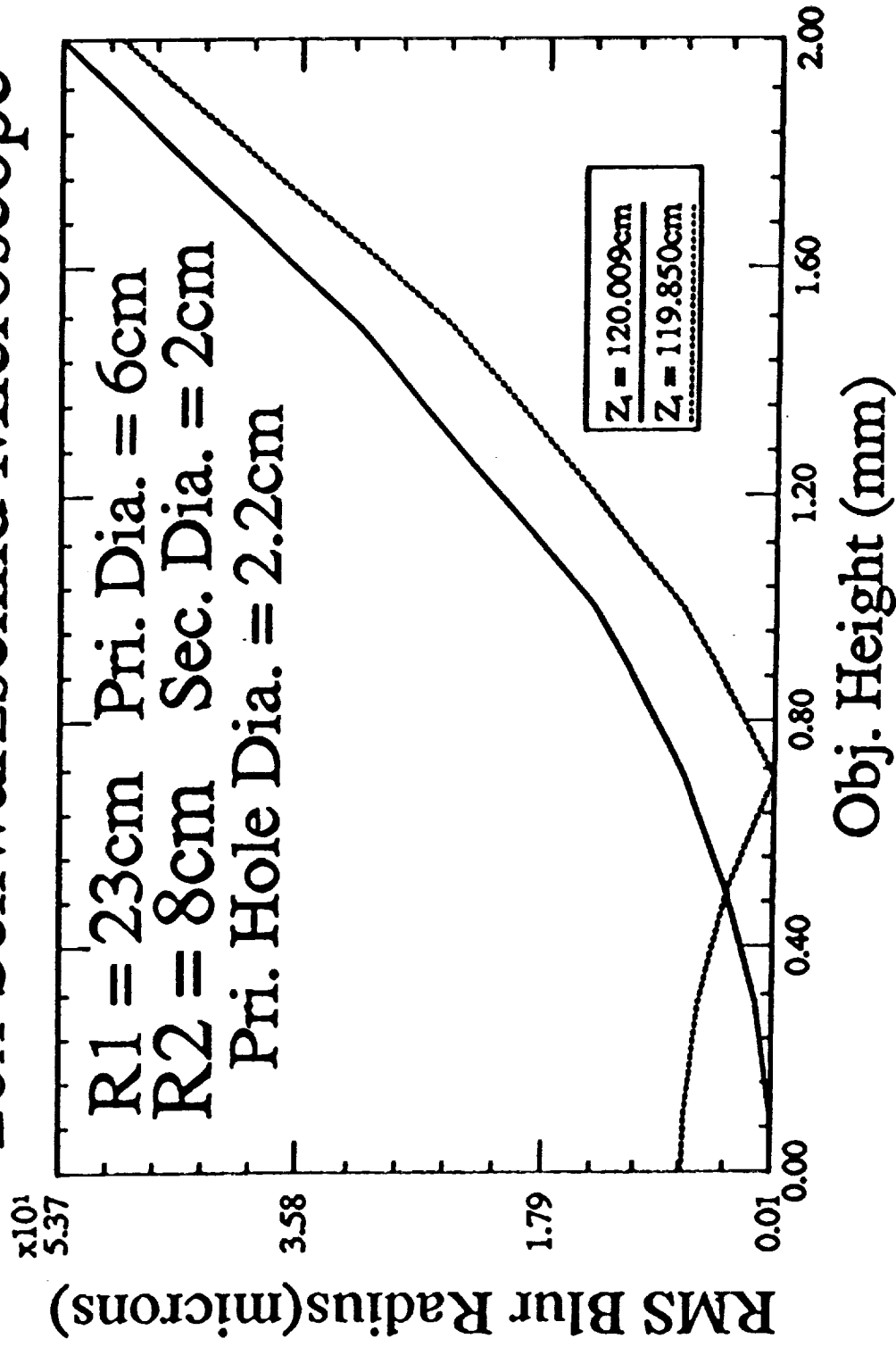


Fig. 9. RMS blur radius vs object height for defocused image planes.

20x Schwarzschild Microscope

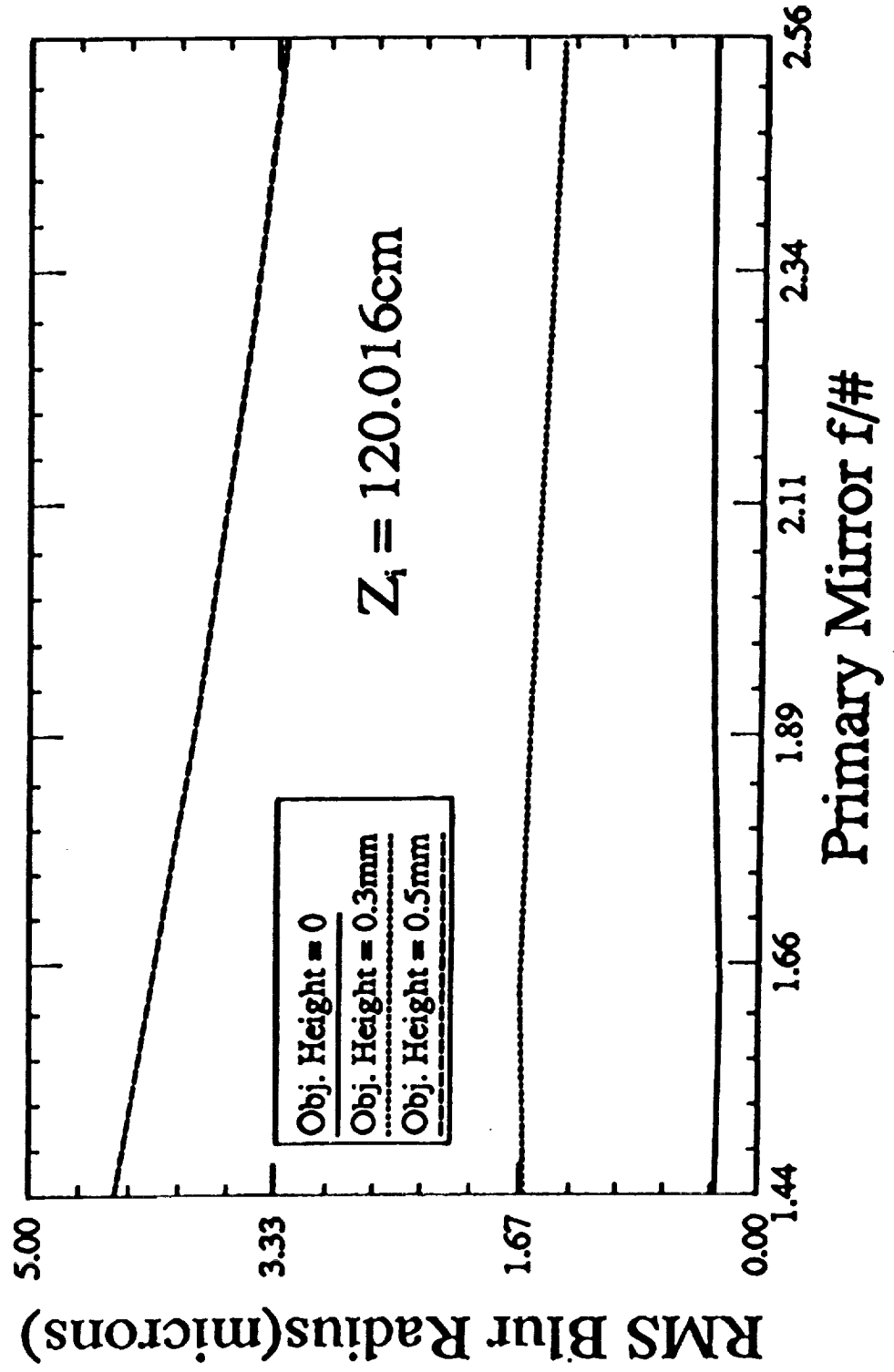


Fig. 10. RMS blur radius vs primary mirror f/# for different object heights.

20x Schwarzschild Microscope

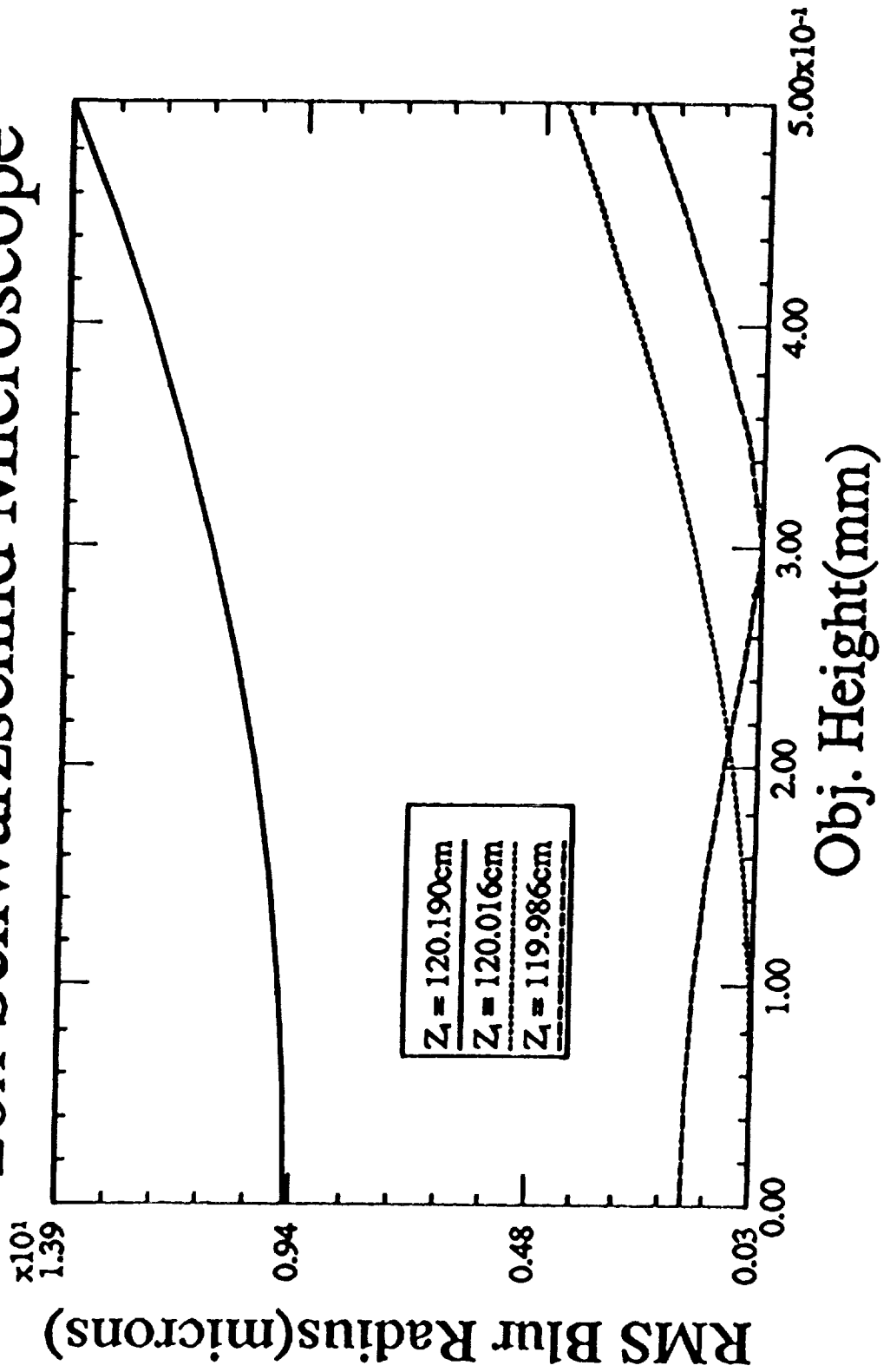


Fig. 11. RMS blur radius vs object height over three image planes.

TABLE 1

Schwarzschild Mirror Parameters

| M(x) | R ₁ (cm) | R ₂ (cm) | s (cm) | d (cm) | Z (cm) | f (cm) |
|------|---------------------|---------------------|--------|--------|--------|--------|
| 2 | 108.00 | 10.00 | 18.25 | 98.00 | -91.42 | 5.51 |
| 3 | 58.27 | 10.00 | 18.05 | 48.27 | -34.12 | 6.04 |
| 4 | 45.58 | 10.00 | 18.01 | 35.58 | -13.56 | 6.41 |
| 5 | 40.00 | 10.00 | 18.00 | 30.00 | 0.0 | 6.67 |
| 10 | 31.79 | 10.00 | 18.02 | 21.79 | 48.36 | 7.29 |
| 15 | 29.69 | 10.00 | 18.04 | 19.69 | 91.04 | 7.54 |
| 20 | 28.75 | 10.00 | 18.05 | 18.75 | 131.49 | 7.67 |
| 30 | 27.84 | 10.00 | 18.06 | 17.84 | 213.27 | 7.80 |
| 40 | 27.40 | 10.00 | 18.07 | 17.40 | 296.07 | 7.87 |
| 50 | 27.15 | 10.00 | 18.07 | 17.15 | 376.42 | 7.92 |

TABLE 2
Schwarzschild Microscope System Parameters

| | |
|------------------------------------|-----------|
| Magnification | 20x |
| Focal Length | 6.133 cm |
| Primary Mirror | |
| Radius of Curvature | 23.0 cm |
| Outside Diameter | 8.0 cm |
| Hole Diameter | 2.2 cm |
| Secondary Mirror | |
| Radius of Curvature | 8.0 cm |
| Outside Diameter | 2.0 cm |
| Object Distance from Secondary (s) | 14.44 cm |
| Mirror Spacing (d) | 15.0 cm |
| Image Distance from Primary (Z) | 105.19 cm |
| Overall Length (s+d+Z) | 134.53 cm |

Author Biographies

David L. Shealy is professor and chair of the Department of Physics at the University of Alabama at Birmingham. He has designed a variety of x-ray telescopes and microscopes for NASA, and is currently working with Los Alamos National Laboratory on the design of soft x-ray grazing incidence free electron laser (FEL) cavities and application of soft x-ray FELs to projection lithography. Dr. Shealy has published a number of papers in x-ray and laser optics, caustic theory, and optical design, and is a fellow of the Optical Society of America.